ICARUS 61, 461–489 (1985)

Remote Sensing of Lunar Pyroclastic Mantling Deposits

LISA R. GADDIS[1] AND CARLE M. PIETERS

Department of Geological Sciences, Brown University, Providence, Rhode Island 02912

AND

B. RAY HAWKE

Hawaii Institute of Geophysics, Planetary Geosciences Division, 2525 Correa Road, Honolulu, Hawaii 96822

Received August 13, 1984; revised November 26, 1984

Mantling deposits on the Moon are considered to be pyroclastic units emplaced on the lunar surface as a result of explosive fire fountaining. These pyroclastic units are characterized as having low albedos, having smooth fine-textured surfaces, and consisting in part of homogeneous, Fe-bearing volcanic glass and partially crystallized spheres. Mantling units exhibit low returns on depolarized 3.8-cm radar maps, indicating an absence of surface scatterers in the 1- to 50-cm-size range. A number of reflectance spectra from several regional pyroclastic deposits are presented for the first time; these data support a previous interpretation that mantling units have a unique spectral signature which is indicative of the presence of a significant Fe-bearing volcanic glass component. The Rima Bode region is discussed as an example of an area in which several types of remote sensing data (including 3.8-cm radar, spectral reflectance, and multispectral vidicon data) were used to reconstruct the geologic events surrounding the emplacement of a regional pyroclastic mantling deposit. The recognition of numerous varieties of volcanic glass samples, especially relatively high-albedo (e.g., green, yellow) glasses, suggests the existence of additional, unrecognized mantling deposits with albedos higher than those studied to date. On the basis of the remote sensing data summarized and presented, five new areas have been identified which may represent higher-albedo regional pyroclastic deposits.

INTRODUCTION

Lunar pyroclastic mantling deposits are thought to form as products of fire fountains which occur in association with basaltic eruptions (e.g., Heiken *et al.*, 1974). Commonly observed in highland areas adjacent to several of the major mare-filled impact basins, these units are likely to mark the locations of source vents for these and earlier volcanic deposits. Volcanic glass spherules, believed to be relatively unfractionated samples of the deep lunar interior (from depths of about 300 km or greater; Delano and Livi, 1981a), are important components of sampled pyroclastic mantling deposits. In contrast to the volatile-depleted bulk lunar composition (e.g., Ganapathy and Anders, 1974), these glasses have surface coatings of relatively high concentrations of volatile elements (Chou *et al.*, 1975; Meyer *et al.*, 1975; Wasson *et al.*, 1976; Butler, 1978; Delano, 1979). The presence of these surface-correlated volatiles, presumably condensed from gases involved in an explosive eruption, suggests the existence of volatile-enriched magma reservoirs within the Moon (Delano *et al.*, 1980; Delano and Livi, 1981b). A clearer understanding of the nature of lunar pyroclastic mantling deposits can thus help to constrain hypotheses concerning the composition of their source material as well as explosive eruption mechanisms on the Moon.

A variety of remote sensing observations

[1] Now at the Hawaii Institute of Geophysics, Planetary Geosciences Division, 2525 Correa Road, Honolulu, Hawaii 96822.

0019-1035/85 $3.00

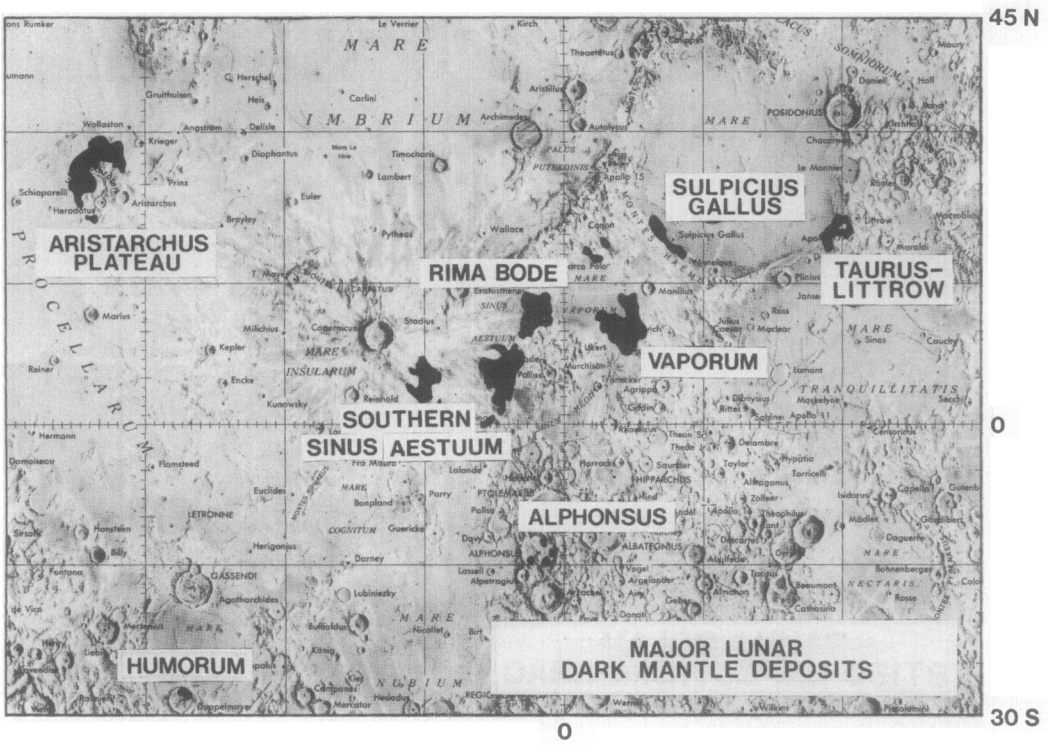

FIG. 1. The distribution of major lunar dark mantle deposits (after Head, 1974). These pyroclastic deposits were recognized primarily on the basis of their low albedos and their mantling relationship to underlying terrain.

have provided much of our current information on the distribution, morphology, and physical characteristics of lunar pyroclastic mantling deposits. These deposits are commonly recognized in the form of regional "dark mantle" deposits widely scattered over the nearside of the Moon (Fig. 1). Observable through Earth-based telescopes, these units have been characterized as extensive deposits of low albedo (0.079–0.096; Pohn and Wildey, 1970) which appear to subdue or mantle underlying terrain (e.g., Carr, 1966). Visual observations and photographs obtained during the Apollo missions indicate that the surface of lunar pyroclastic materials is relatively fine-textured, with a smooth, velvety appearance (Fig. 2; Cernan *et al.*, 1972; Lucchitta, 1973; Lucchitta and Schmitt, 1974). Low returns on Earth-based 3.8-cm depolarized radar backscatter maps confirm these observations of mantled areas, indicating an absence of surface scatterers in the 1- to 50-cm-size range (Pieters *et al.*, 1973; Zisk *et al.*, 1974).

Our understanding of the chemistry and mineralogy of unsampled lunar basaltic materials has been greatly increased by remote sensing observations calibrated using samples returned from the Moon (e.g., Adams and McCord, 1970, 1971, 1972; Adams, 1974; Andre *et al.*, 1977; Arnold *et al.*, 1977; Bielefeld *et al.*, 1977; Pieters, 1978; Schonfeld and Bielefeld, 1978). While a probable pyroclastic mantling deposit at Taurus–Littrow has indeed been sampled (e.g., LSPET, 1973), such "ground truth" does not exist for many other similar units. Further data on these pyroclastic deposits are currently limited to those obtainable by remote observation.

The purposes of this paper are to summa-

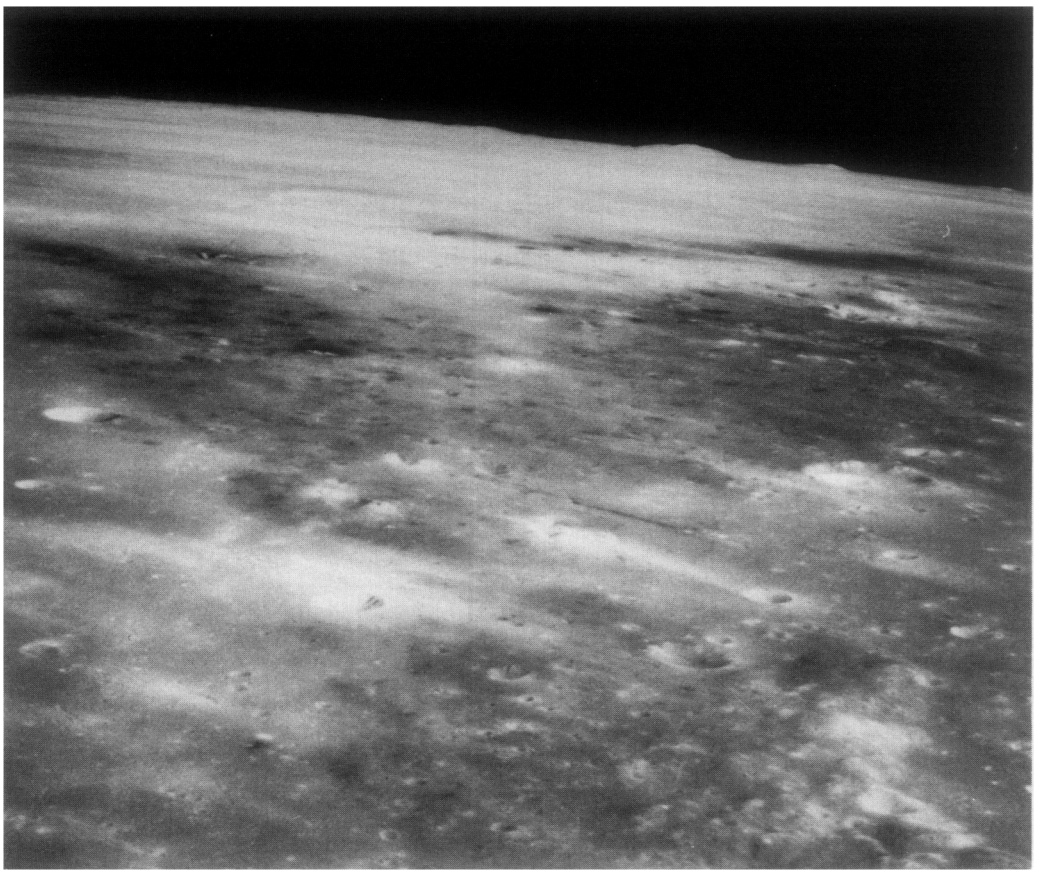

FIG. 2. This Apollo 12 panorama shows an oblique view of the low-albedo pyroclastic mantling deposit in southern Sinus Aestuum. The larger crater of the nested-crater pair to the right is approximately 10 km in diameter. The view is north toward the Apennine Mountains (NASA AS12-52-7732).

rize current morphological, 3.8-cm radar, and spectral reflectance data for lunar pyroclastic mantling deposits. Analyses and interpretation of representative reflectance spectra of several pyroclastic deposits, presented here for the first time, demonstrate that lunar mantling deposits have unique signatures which are indicative of the presence of a significant component of volcanic Fe-bearing glass. In addition, to substantiate the utility of remote sensing data as a tool for characterizing regional lunar mantling deposits, we present an analysis of the Rima Bode region of the Moon; remote sensing data for this area have been used extensively to interpret its geologic history. Finally, the recognition of numerous samples of volcanic glass, especially relatively high-albedo (e.g., green, yellow) glasses, suggests the existence of additional, unrecognized mantling deposits with albedos higher than those studied to date. We have utilized the low depolarized 3.8-cm radar signature of recognized regional mantling deposits to identify five areas which may represent such higher-albedo regional pyroclastic deposits.

LUNAR PYROCLASTIC MANTLING DEPOSITS: BACKGROUND INFORMATION

Several major occurrences of regional lunar dark mantle deposits have been documented (e.g., Carr, 1966; Wilhelms, 1970; Wilhelms and McCauley, 1971), including

those at the following locations: Taurus–Littrow (Lucchitta, 1973; Pieters *et al.*, 1973, 1974), Sulpicius Gallus (Lucchitta and Schmitt, 1974; Head *et al.*, 1980; Schonfeld, 1981), Mare Humorum (Pieters *et al.*, 1975), Aristarchus (Zisk *et al.*, 1977), Palus Putredinis (Hawke *et al.*, 1979), and Rima Bode (Wilhelms, 1968; Gaddis *et al.*, 1981). In each of these regions, mantling material is generally concentrated in highland areas adjacent to a major mare-filled basin. This spatial proximity, in conjunction with data for Apollo 17 samples which indicate similar formation ages for orange glasses (approximately 3.65 by; Huneke, 1978; Alexander *et al.*, 1980) and subfloor basalts (3.71 to 3.83 by; summarized by Heiken *et al.*, 1974) at Taurus–Littrow, supports an association between the mantling materials and nearby mare deposits. Head (1974) noted that if associated mare flows were subsequently covered by younger mare deposits, evidence of the location and composition of earlier mare deposits should exist in the form of remnant mantling material on the uplands. An understanding of the distribution of regional lunar mantling deposits could therefore be useful in the determination of the stratigraphy of many of the lunar maria.

The observed regional pyroclastic deposits may be distinguished from a second, more localized type of volcanic mantling deposit which has been recognized on the Moon. Deposits associated with the endogenic dark-halo craters of Alphonsus are representative of this localized lunar mantling material. The Alphonsus dark-halo craters are typically small (on the order of 2 km across) and noncircular, aligned along floor fractures, and surrounded by halos of low-albedo material of inferred pyroclastic origin (Head and Wilson, 1979); individual halos range up to 80 km^2 in areal extent. These volcanic craters have been distinguished from impact-produced dark-halo craters on the basis of their noncircularity, reduced crater depth-to-diameter ratio, absence of rays, unusually smooth, untextured peripheral deposits, and spectral reflectance characteristics (Head and Wilson, 1979; Hawke and Bell, 1981). Since it is not known whether localized deposits have been sampled on the Moon, we have no direct indication that glasses are major components of these pyroclastic units.

Eruption conditions of regional and localized lunar pyroclastic materials have been inferred from observations of mantling deposit and source vent morphologies (Wilson and Head, 1981). The presence of volatile-element coatings on the volcanic glasses in samples returned from regional deposits strongly suggests the existence of a gas phase in their source magmas. Calculations by Wilson and Head (1981) show that a regional pyroclastic deposit and possible associated lavas can be produced by a continuous eruption of lunar magma with gas present; the areal extent of such a deposit varies directly with the gas content of the magma and its mass eruption rate (McGetchin and Ullrich, 1973). Sinuous rilles and irregular depressions, both commonly associated with regional mantling deposits, are inferred to be source vents for these pyroclastic units (Basaltic Volcanism Study Project, 1981, Chap. 5, p. 760). By contrast, the distinctive morphology of the localized Alphonsus-type mantling deposits points to an eruption mechanism analogous to that observed for vulcanian explosive activity on Earth (Head and Wilson, 1979). In this case, accumulation of gas in a capped magma conduit promotes explosive decompression, resulting in the localized distribution of fine-grained pyroclastic materials (a "halo") around an endogenic source crater.

An important objective of the Apollo 17 mission was to sample the "dark mantle" deposit at Taurus–Littrow; premission analysis indicated that this deposit might be of pyroclastic origin (Scott *et al.*, 1972). Orange glass droplets and partially crystallized black spheres from the Apollo 17 landing site were subsequently identified as pyroclastic components of this deposit

(Heiken *et al.*, 1974). Physical, chemical, and petrographic characteristics which have been cited as evidence for the pyroclastic origin of lunar volcanic glasses include (1) major-element chemical uniformity among individual volcanic glasses; (2) uniform Ni abundances within individual samples and within compositional groups; (3) high Mg/Al ratios; (4) presence of euhedral olivine phenocrysts; (5) absence of schlieren, exotic inclusions, shocked debris, surficial iron grains, or other features considered to be indicative of an impact origin; (6) presence of composite and/or partially crystallized droplets interpreted as fallback material from a fire fountain; and (7) concentrations of volatile elements on sphere surfaces by a vapor condensation mechanism (Heiken *et al.*, 1974; Schonfeld and Bielefeld, 1978; Butler, 1978; Delano and Livi, 1981b; Stone *et al.*, 1982).

To date, 23 varieties of lunar volcanic glasses (forming two chemical arrays) have been identified, including Apollo 11, 14, 15, and 16 green glasses, and Apollo 14, 15, and 17 yellow glasses (Delano and Livi, 1981b; Delano and Lindsley, 1983a,b). The number of groups is expected to increase when samples from Apollo 12, Luna 16, 20, and 24 have been more thoroughly examined. Specific pyroclastic deposits with which many of these volcanic glasses could be associated have yet to be identified.

REMOTE SENSING CHARACTERISTICS OF LUNAR PYROCLASTIC MANTLING DEPOSITS

Pyroclastic mantling deposits are unique among lunar volcanic materials. The fire-fountain origin of their volatile-coated pyroclastic material stands in striking contrast to the massive outpouring of volatile-depleted, low-viscosity magma which formed the lunar maria and is considered representative of the style of lunar eruptive activity. Their proximity to and probable association with some of the early lunar mare deposits suggests that mantling deposits may have formed during the early stages of eruptive activity. An examination of their morphologies and distribution may therefore lead to a better understanding of the locations of the source vents of these early lunar eruptions. The distinctive 3.8-cm radar and spectral characteristics of lunar pyroclastic mantling deposits can provide information which is particularly relevant to such an undertaking.

Radar

The delay-Doppler technique has been used to obtain Earth-based radar reflectivity measurements of the surface of the lunar nearside (e.g., Pettengill *et al.*, 1974). Both polarized and depolarized components have been measured at a number of radar wavelengths; of these, 3.8-cm wavelength radar, with about 2-km resolution, is most sensitive to small-scale roughness (about 1 to 50 cm; Zisk *et al.*, 1974). Two major factors have been interpreted as controlling lunar radar backscatter: local slope and the relative amount of diffuse components (Thompson and Zisk, 1972). Topographic features facing toward or away from the radar beam produce highlights or "shadows," respectively, on the radar map. In areas in which local slopes are not responsible for differences in echo strength, diffuse scattering, controlled in part by the presence of surface scatterers (rocks, boulders, etc.) 1 to 50 cm in size and by bulk electromagnetic properties (dielectric constant, loss tangent, etc.), is considered to be dominant (Thompson, 1979). Returns on depolarized radar maps range from the enhanced values characteristic of "fresh," blocky craters (Thompson *et al.*, 1974) to the low returns of smooth-surfaced regional pyroclastic mantling deposits (Pieters *et al.*, 1973).

All recognized regional mantling deposits on the lunar surface are distinguished by very weak to nonexistent echoes on the depolarized 3.8-cm radar maps of Zisk *et al.*, (1974). These low depolarized returns are thought to be due to the lack of scatterers on the smooth surfaces of pyroclastic mantling deposits (Pieters *et al.*, 1973; Zisk *et*

al., 1977). Low depolarized returns on 3.8-cm radar maps have been used by a number of workers to map the areal extent of pyroclastic units (e.g., Pieters *et al.*, 1975; Zisk *et al.*, 1977; Hawke *et al.*, 1979; Gaddis *et al.*, 1981). As observed at Rima Bode (discussed in detail below), the gradational nature of the contact between pyroclastic deposits and surrounding units is often exhibited on depolarized 3.8-cm radar maps in the form of mottled, low to moderate backscatter as mantling material thins outward. The utility of 3.8-cm radar backscatter data in identifying and characterizing lunar pyroclastic mantling deposits is discussed further in later sections.

Spectral Reflectance

Remotely obtained spectral reflectance measurements can be used to derive geochemical and mineralogical information from the soils that cover much of the surface of the Moon. A prominent feature of all lunar reflectance spectra is the positive continuum slope (i.e., an overall increase in reflectivity toward longer wavelengths; e.g., McCord *et al.*, 1972). Mineral fragments in lunar soils produce residual absorption features which are superimposed on this positive continuum. The energy of these absorption bands (measured in wavelengths) is determined by the electronic configuration of transition element ions (e.g., Fe^{+2}, Fe^{+3}, Ti^{+3}, Ti^{+4}) and by the geometry of the coordination sites of their host minerals (Burns, 1970a). The dominant absorption feature for lunar materials has a wavelength centered near 1.0 μm and is primarily due to Fe^{+2} crystal field transitions in distorted octahedral coordination sites. This 1.0-μm band has four major mineral contributors in lunar soils: orthopyroxene, clinopyroxene, olivine, and Fe-bearing volcanic glasses. Volcanic glasses must be distinguished from impact-produced agglutinitic glasses which are common in mature lunar soils. Bell *et al.* (1976) have shown that laboratory spectra of homogeneous synthetic glasses contain distinct Fe^{+2} absorption features; these synthetic glasses are considered to be suitable analogs for quenched lunar volcanic glasses. By contrast, the presence of agglutinates and/or opaque components (e.g., ilmenite, Fe metal) in lunar soils serves to lower their spectral contrast, increasing the continuum slope and reducing the strength of absorption features contributed by lithic fragments (e.g., Adams and McCord, 1971; Charette *et al.*, 1976). Since the use of reflectance spectroscopy in identifying pyroclastic deposits requires the distinction of these four possible components, a more detailed summary of their spectral properties is presented below.

Orthopyroxene exhibits two absorption bands, centered between 0.90 to 0.94 μm and 1.8 to 2.1 μm (Adams, 1974; Hazen *et al.*, 1978), and is a major mafic mineral associated with lunar highland materials. A laboratory reflectance spectrum for a mature highland soil sample returned by Apollo 16 is presented in Fig. 3. The nearly symmetric absorption band centered near 0.90 μm is due to orthopyroxene fragments in the sample. Additional information concerning this spectrum and others discussed in this paper are presented in Table I.

Longer-wavelength absorption bands centered near 0.95 to 1.0 μm are characteristic features of spectra of the lunar maria and are due to the more calcium-rich clinopyroxene in the soils. Examples of Earth-based telescopic reflectance spectra of two mature lunar maria (Apollo 17 and Mare Serenitatis 2) are also presented in Fig. 3. Although both mare soil spectra exhibit absorption bands attributable to clinopyroxene, there are obvious differences in the way these bands are manifested. The absorption feature on the Apollo 17 spectrum (at 0.98 μm) is relatively shallow and weak compared to the strong clinopyroxene band (at 1.0 μm) on the more steeply sloped Mare Serenitatis 2 (MS-2) spectrum. The difference in absorption band strength of these two basaltic units is largely due to differences in spectral contrast, which in

TABLE I

LOCATION OF LUNAR AREAS FROM WHICH SPECTRAL REFLECTANCE MEASUREMENTS WERE OBTAINED

Atlas Designation[a]	Coordinates	Date Observed	Surface Unit
Apollo 16	9.0 S, 15.1 E	All nights	Sampled highland soil
Apollo 17	19.7 N, 30.6 E	7-30-80	High-Ti mare
Mare Serenitatis 2	18.7 N, 21.4 E	7-14-81	Low-Ti mare
Littrow 1	20.6 N, 29.7 E	9-14-81	Mantled mare
Sinus Aestuum 2	12.5 N, 3.0 W	6-30-80	Mantled highlands
Sulpicius Gallus 2	20.4 N, 9.7 E	9- 5-79	Mantled highlands
Mare Humorum MM	26.7 S, 44.3 W	9-16-81	Mantled mare
Aristarchus Plateau 1	27.1 N, 52.8 W	8- 3-80	Mantled highlands
Sinus Aestuum 6	7.8 N, 1.4 W	6-30-80	Unmantled highlands
Rima Bode mare	11.7 N, 6.0 W	6-30-80	Unmantled mare (Sinus Aestuum)
Sinus Aestuum 3	10.8 N, 3.2 W	6-30-80	Unmantled mare ("perched")

Note. All data were calibrated using Apollo 16 soil sample 62231; no thermal corrections have been made for these measurements.

[a] Atlas compiled by Pieters and Smrekar, 1982.

turn is dependent on the variation in titanium content between the two mare soils. The Apollo 17 mare soils have an average TiO_2 concentration of about 9%, while soils from the MS-2 area are estimated to have less than 3% TiO_2 (Pieters, 1978). The direct dependence of spectral contrast on TiO_2 content is a complex relationship involving absorption due to charge transfers between Fe and Ti in mare soils, and absorption and scattering by agglutinitic opaques. For mature mare soils, lower TiO_2 content is associated with higher spectral contrast, which allows absorption features to be observed more prominently.

The characteristic Fe^{+2} absorption band of olivine is superficially similar to a homogeneous Fe-bearing glass band—both are broad, relatively weak, and centered slightly beyond 1.0 μm. Olivine, however, has a higher overall albedo than Fe–Ti-bearing glasses, and its 1.0-μm Fe^{+2} feature is, in fact, a composite of three distinct, superimposed absorption bands (Burns, 1970b; 1974). Laboratory studies of mineral mixtures indicate that the characteristic olivine 1.04-μm absorption band is obscured by pyroxene absorption bands unless the sample is more than approximately 70% olivine (Singer, 1981). The presence of olivine can nevertheless be detected at lower levels of concentration by distortions to the long-wavelength edge of the pyroxene band. Olivine has been observed as a major mafic component in some moderate- to high-albedo areas on the Moon (e.g., the central peak of Copernicus; Pieters, 1982).

Although, as Farr *et al.* (1980) have suggested, it may be justified to assume that impact-produced agglutinitic glasses produce no major absorption bands in mare soils, spectral contributions from Fe-bearing volcanic glasses cannot be neglected. Distinctive, broad absorption bands near 1.1 μm of Fe-bearing, homogeneous volcanic glasses have been observed in laboratory spectra of both returned lunar pyroclastic samples, such as Apollo 17/Taurus–Littrow orange glasses and Apollo 15 green glasses (Adams *et al.*, 1974), and a suite of simulated lunar Fe–Ti glasses (Bell *et al.*, 1976). Detection of a glass band near 1.0 μm in remote lunar spectra would therefore suggest a significant concentration of Fe-bearing glasses of a probable pyroclastic origin in the soils (as at Aristarchus; Zisk *et al.*, 1977; Hawke *et al.*, 1983).

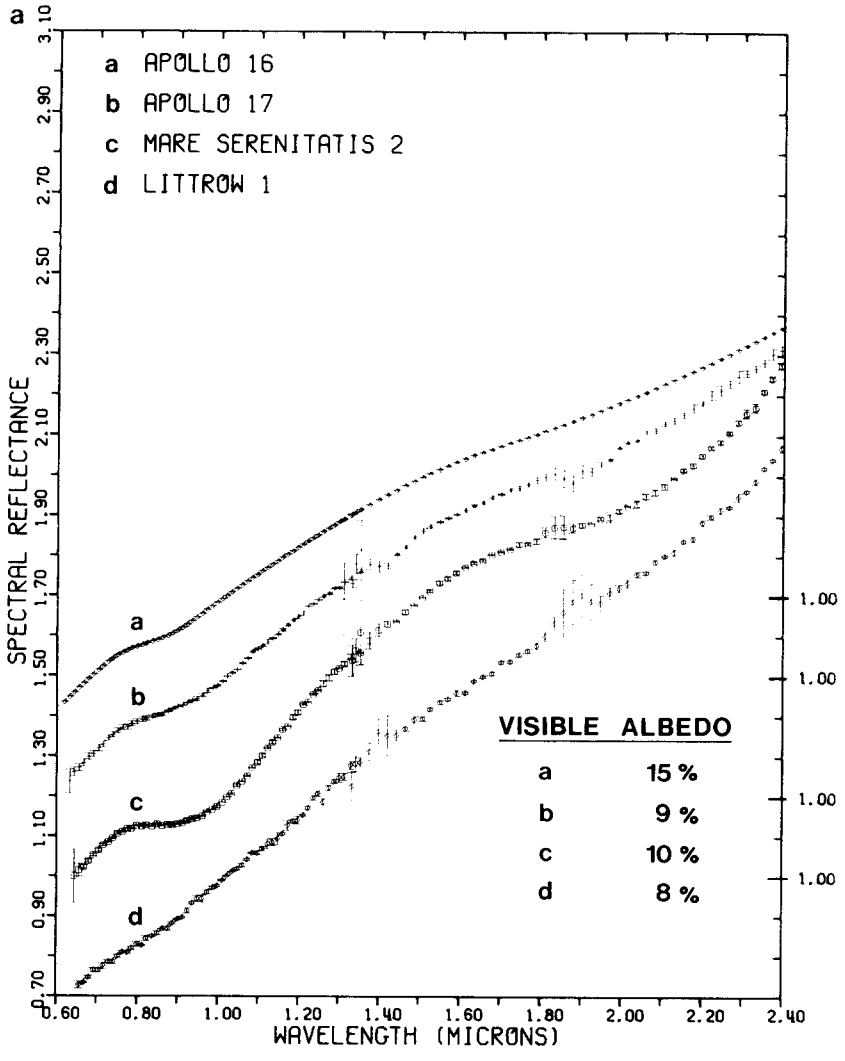

FIG. 3. (a) Spectral reflectance measurements of representative areas of the lunar surface; each has been scaled to unity at 1.02 μm and offset relative to adjacent spectra. (b) Residual absorption features for the same measurements after a straight-line continuum (through 0.73 and 1.6 μm) has been removed.

Near-infrared reflectance spectra for a number of regional "dark mantle" deposits were obtained at the 2.2-m University of Hawaii telescope facility on Mauna Kea, Hawaii, and processed according to the methods outlined by McCord *et al.* (1981). Several of these spectra, presented here for the first time, are shown in Fig. 4. The remote reflectance spectrum from the pyroclastic deposit at Taurus–Littrow (Littrow 1 in Figs. 3 and 4) has a very steep continuum slope and a broad, very shallow 1.0-μm absorption band. The spectral contrast of the Littrow 1 spectrum is even more reduced than that of the Apollo 17 high-titanium mare deposit spectrum. Laboratory reflectance measurements of samples returned by Apollo 17 show that the dark crystallized spheres from Station 4 on the rim of Shorty Crater are the characteristic

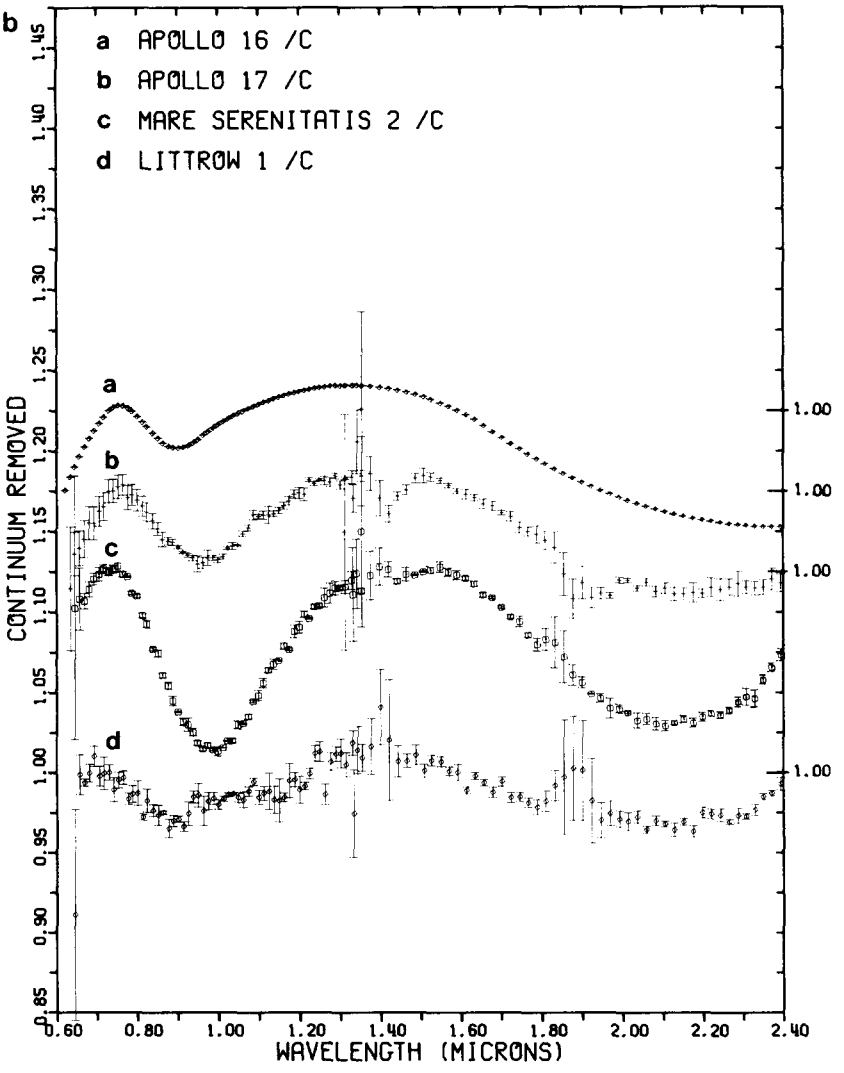

FIG. 3—*Continued.*

ingredients of the Taurus–Littrow mantling deposit (Pieters *et al.*, 1974). The black volcanic spheres which dominate spectra of the Taurus–Littrow mantling material are nearly opaque, devitrified chemical equivalents of the homogeneous Fe–Ti orange glasses (Heiken *et al.*, 1974). These unique black spheres have apparently reduced the spectral contrast of soil developed on the Taurus–Littrow pyroclastic deposits even more than the normal buildup of agglutinates during soil maturation.

Examination of reflectance and continuum-removed spectra for several unsampled dark-mantling deposits (Fig. 4) reveals that all have broader, longer-wavelength absorption bands than those which can be attributed to pyroxenes alone in highland and mare soils. There must be an additional, Fe-bearing soil component which has both modified this 1.0-μm band and maintained the low albedo of the materials observed. Our preferred interpretation is that absorptions by Fe-bearing volcanic

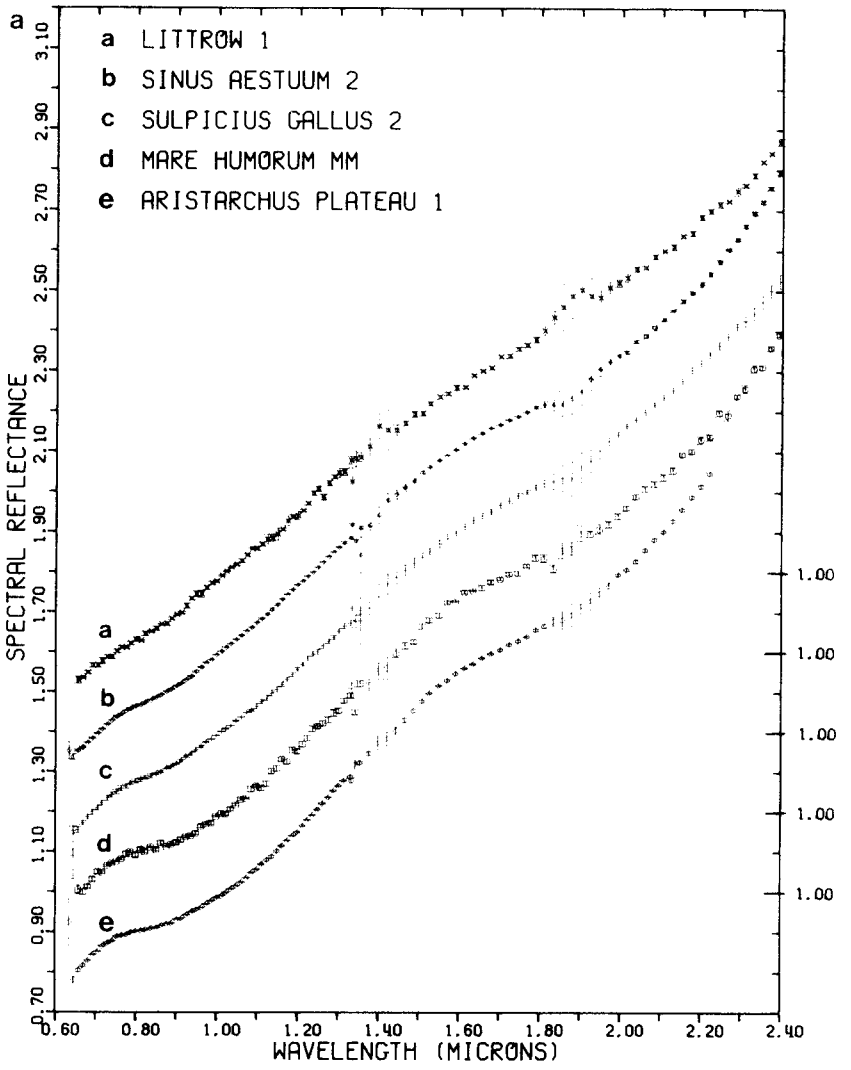

FIG. 4. (a) Scaled spectral reflectance measurements of several unsampled lunar regional pryoclastic deposits. The spectrum for Littrow 1, the area near the deposit at Apollo 17/Taurus–Littrow, has been reproduced for comparison. (b) Residual absorption features for the same measurements after continuum removal.

glasses have produced the 1.0-μm bands in these spectra. Although spectral contributions from olivine cannot be discounted, the observed albedos of these mantled areas would not be among the lowest on the lunar surface if olivine alone was responsible for these strong 1.0-μm absorption bands. The presence of Fe-bearing volcanic glasses in the mantling deposits from which these spectra were obtained is therefore most consistent with our evidence.

AN APPLICATION OF REMOTE SENSING DATA TO THE CHARACTERIZATION OF LUNAR PYROCLASTIC MANTLING DEPOSITS

Although analysis of remote sensing data can provide important information concerning the physical nature, areal extent,

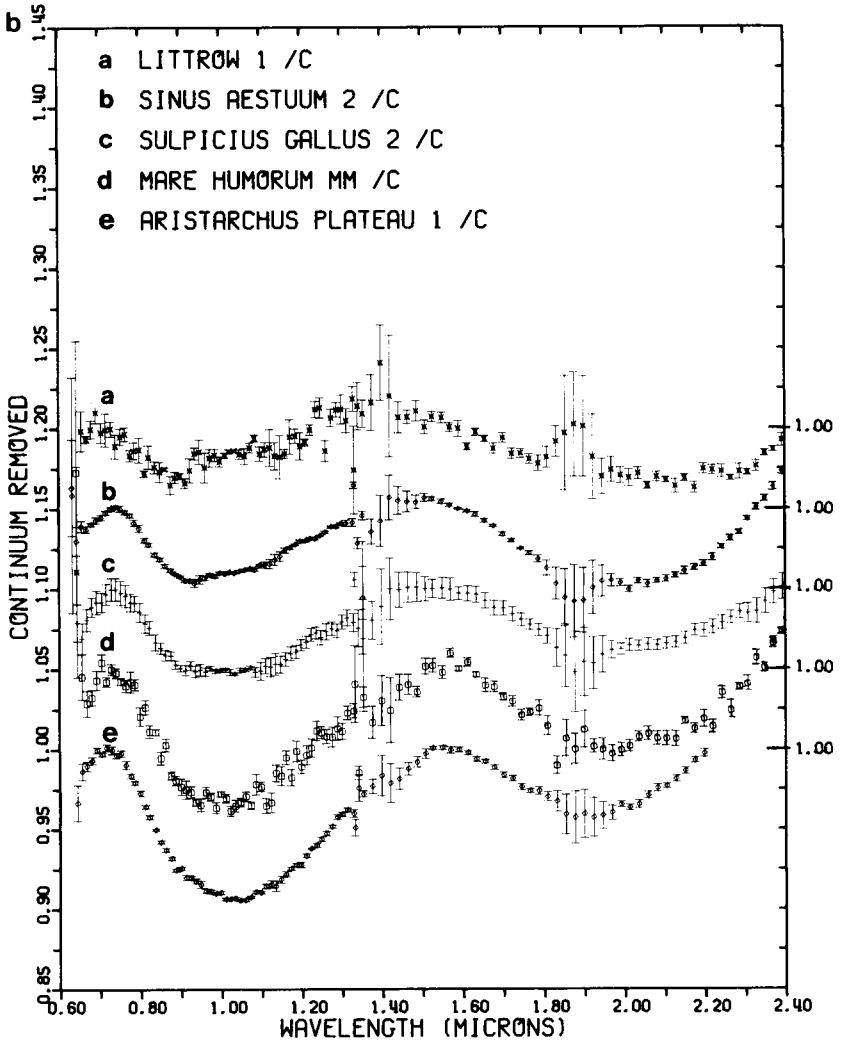

FIG. 4—*Continued.*

and composition of lunar mantling deposits, critical evidence in support of their pyroclastic origin is provided by morphological analyses. Specific features of mantling deposits which might be considered diagnostic of such an origin include diffuse boundaries and irregular thicknesses of regional deposits; a localized halo surrounding a crater with an apparent endogenic origin; and the presence of other probable vents (e.g., sinuous rilles, irregular depressions, etc.) and/or associated mare deposits. As an illustration of the integration of diverse data, the following discussion focuses on a specific example in which remote sensing data have been used in conjunction with photogeologic information to investigate a regional lunar mantling deposit.

The Rima Bode Example

Located in the central portion of the lunar nearside, the Rima Bode region is distinguished by a dark blanket of mantling

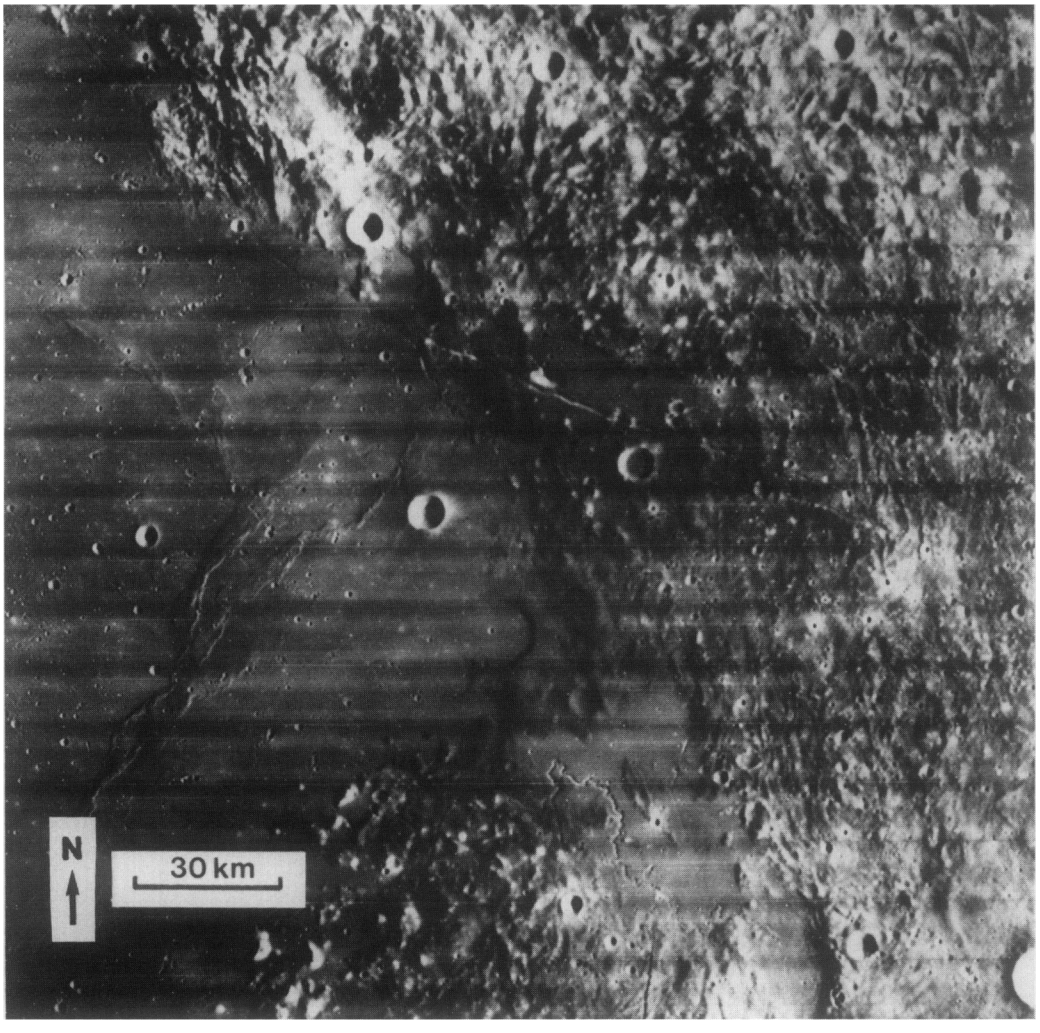

FIG. 5. High-resolution Lunar Orbiter IV (LO IV-109H2) photograph of the Rima Bode region of the Moon.

material which covers a highland area of about 10,000 km^2 between the mare deposits of northern Sinus Aestuum and Mare Vaporum (Figs. 1 and 5; Wilhelms, 1968). The underlying terrain displays the hummocks and lineations characteristic of the Imbrium basin ejecta deposit. Photogeologic, radar, and spectral characteristics of the surface in the Rima Bode region are summarized in Table II. These characteristics were used to identify six geologic units which are illustrated in Fig. 6 (Gaddis *et al.*, 1981).

The Rima Bode pyroclastic mantling deposit can be differentiated into two concentrically occurring units on the basis of low depolarized returns on 3.8-cm radar maps (Fig. 7). The central unit (unit A) is small (about 3600 km^2), has both low albedo and low radar backscatter values, and is apparently continuous. Areas of higher-albedo, enhanced-return material exposed by small impact craters which have penetrated this unit are rare, suggesting that this unit encompasses the area of thickest mantling. The larger surrounding unit (unit B) has a

TABLE II

PHOTOGEOLOGIC, RADAR, AND SPECTRAL CHARACTERISTICS OF RIMA BODE GEOLOGIC UNITS

Unit	Albedo	Morphology	Backscatter	UV/VIS	Band	Interpretation
A	Very low	Continuously mantled terra	Very Low	High	Very weak	Heavily mantled; high-Ti glass spheres
B	Low	Sparsely mantled terra	Low (mottled)	High (mottled)	—	Less mantled; similar to unit A
C	High	Hummocky terra	Moderate	Moderate–low	Weak	Basin ejecta deposits
D	Low	Mantled mare	Low	High	—	Unknown mare; mantled, as are units A and B
E	Moderate	Unmantled mare	Moderate	Moderate	Moderate	Low-Ti basalt
F	Moderate	Unmantled mare	Moderate	Moderate	Weak	Low-Ti basalt

mottled and patchy appearance on both photographs and 3.8-cm depolarized radar images of this area.

There are two rilles in the region (Rimae Bode I and II; Fig. 6), but both are unlikely pyroclastic source vents because they are located along the perimeter of the area of heaviest mantling. Both the northern rille, Rima Bode II, and nearby irregular depressions appear to have been mantled by pyroclastic material (Schultz, 1976, p. 272). Rima Bode II cuts across the nearby mantled mare deposit (unit D) but does not appear to be associated with the source vent for this deposit. By contrast, Rima Bode I is unmantled, sinuous, and appears to be associated with the source vent for the small, unmantled mare deposit (unit F) to the south. This "perched" lava pond of unit F and its associated rille are typical of

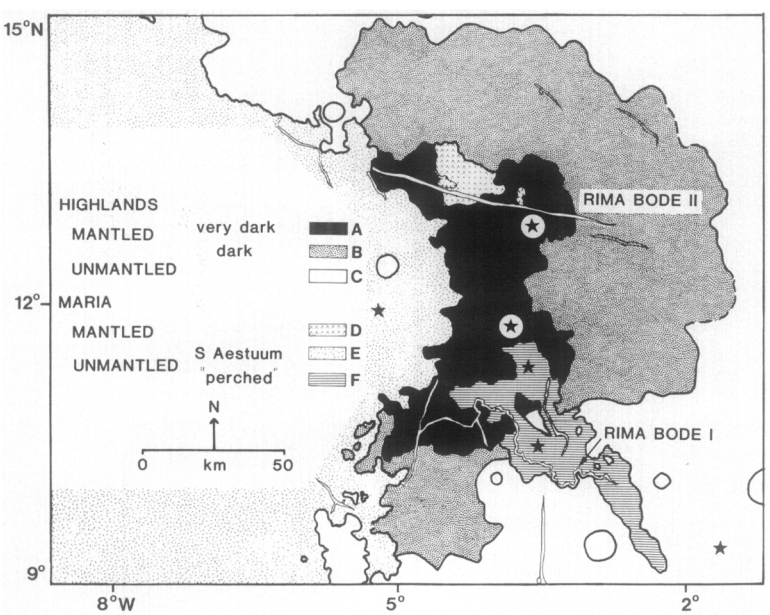

FIG. 6. Distribution of geologic units of the Rima Bode region. Areas from which spectra were obtained are indicated with stars.

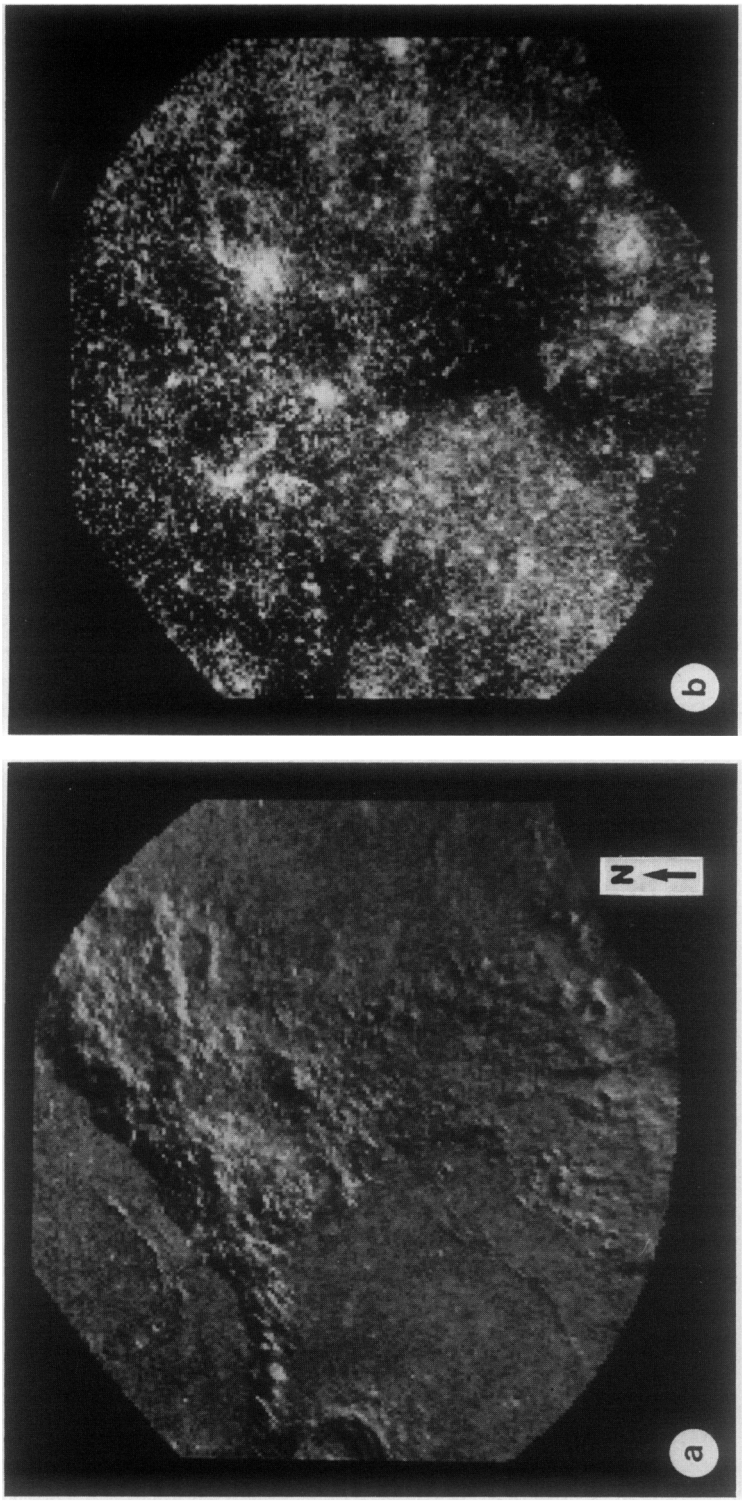

FIG. 7. (a) Polarized and (b) depolarized 3.8-cm radar backscatter maps of Rima Bode (ZAC 2.12; Zisk *et al.*, 1974).

small mare deposits in the highlands, as observed elsewhere on the Moon (e.g., the Orientale region, Gaddis and Head, 1981). The approximately concentric nature of the two units of mantling material (units A and B) suggests that the source vent was located to the west in Sinus Aestuum. Unfortunately, the deposition of later mare deposits in northern Sinus Aestuum has obliterated direct evidence of this vent.

The spectral characteristics of units of the Rima Bode region have been determined from several telescopic near-infrared spectra (0.6 to 2.5 μm; characteristic sites are indicated with stars in Fig. 6) and multispectral images of this area (McCord *et al.*, 1976; Pieters, 1978; Gaddis *et al.*, 1981). Four representative spectra for Rima Bode units are presented in Fig. 8 as scaled spectral reflectance curves and the residual absorptions after a continuum removal. Analyses of the spectral data indicate that (1) although the unmantled mare of Sinus Aestuum (unit E) and the perched lava pond (unit F) both have low 0.40/0.56-μm (UV/VIS) ratios in multispectral images, they are distinguishable from each other on the basis of the strength of the 1.0-μm absorption band (unit F has a weaker band); (2) the central, most heavily mantled pyroclastic unit of Rima Bode (unit A) is spectrally very similar to the dark mantling material of Taurus–Littrow (compare curves Littrow 1 and Sinus Aestuum 2 on Fig. 4a); and (3) the continuum slope and short-wavelength band centers of unmantled highlands (unit C) in this area are similar to those elsewhere on the Moon (e.g., at the Apollo 16 landing site; compare with Fig. 3).

A number of important implications arise from interpretations of these data. First, the low 0.40/0.56-μm ratios of both unmantled maria at Rima Bode (units E and F) are indicative of low titanium contents of surface soils (e.g., Charette *et al.*, 1974; McCord *et al.*, 1976; Pieters, 1978). The compositions of these basalts can be compared to other low-titanium mare deposits which are observed in central Mare Serenitatis, at Apollo 12, and elsewhere on the lunar nearside [these are the moderately "red' maria of Whitaker (1972)]. By contrast, since analysis of spectral reflectance curves of dark mantling material at Taurus–Littrow (calibrated with sample data) indicates that this deposit is primarily composed of iron- and titanium-rich, partially crystallized black spheres (Adams *et al.*, 1974), the pronounced similarities between spectra of mantling deposits from Taurus–Littrow and Rima Bode suggest that the latter is also likely to have a major component of high-titanium, black spheres. The inferred compositional similarities between the Rima Bode and Taurus–Littrow pyroclastic materials emphasize the nonuniqueness of the latter and suggest that other such chemically similar deposits may exist on the lunar surface. The occurrence of similar high-titanium volcanic glasses in samples collected from widely separated Apollo landing sites (e.g., the orange glasses from Apollo 11, 14, 15, and 17; Delano and Livi, 1981b) supports this statement. If, as suggested for the Apollo 17 site (Head, 1974), the emplacement of pyroclastics in the Rima Bode area was associated with high-titanium volcanism, then mare basalts of similar compositions would underlie the low-titanium maria (unit E) currently observable in Sinus Aestuum. This suggestion is supported by spectral reflectance data which indicate that the dark-halo crater Copernicus H, located in the ejecta blanket east of Copernicus, penetrated the surficial low-titanium basalts just southwest of Sinus Aestuum and excavated underlying high-titanium basalt (Pieters, 1977).

The spectra of mantling deposits at Rima Bode suggest that these units have been relatively unaffected by contamination from either mare basalt or highland materials. The similar spectral signatures of the pyroclastic deposits of Rima Bode (deposited mainly upon highlands) and Taurus–Littrow (deposited largely upon mare material) precludes the possibility of significant verti-

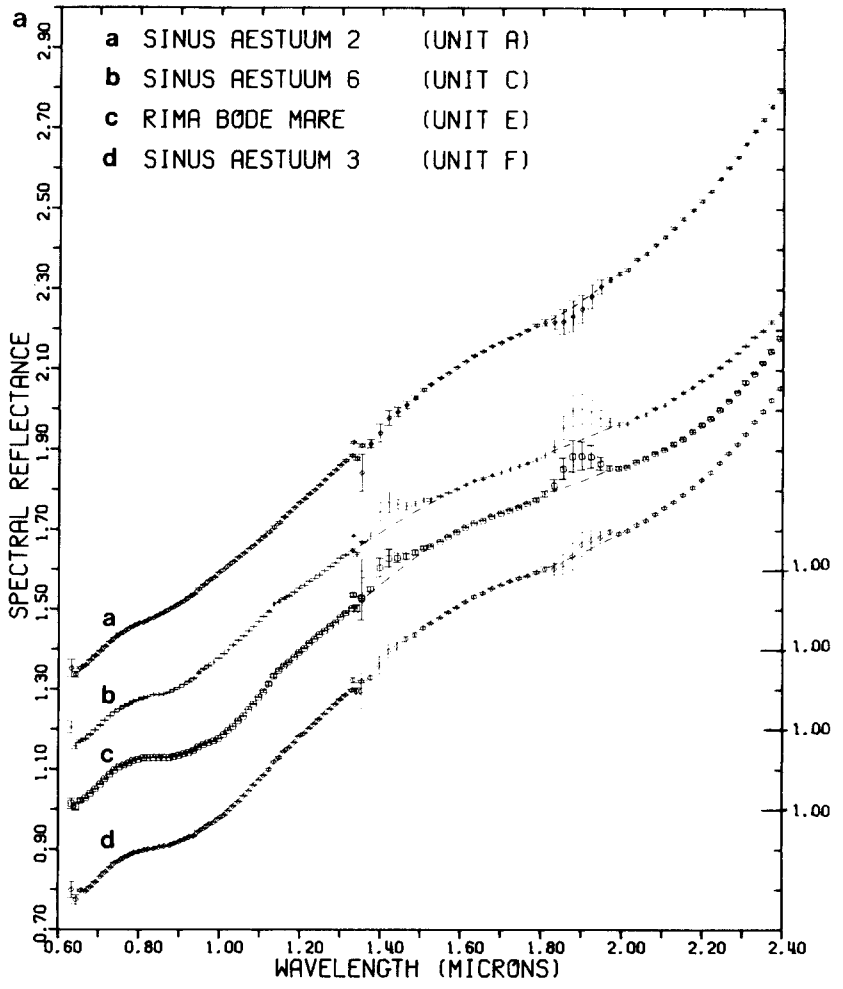

FIG. 8. (a) Scaled spectral reflectance and (b) residual absorption data from Rima Bode geologic units. Continuations of the data in areas of absorption by atmospheric water are estimated with dashed lines.

cal mixing with the substrate. In addition, the possibility of horizontal mixing at Rima Bode is limited by the sharpness of the contacts between both the younger unmantled mare surface (e.g., unit F) and the mantled highlands.

In summary, the stratigraphic history of the Rima Bode area includes the deposition of high-titanium pyroclastic mantling materials (units A and B) upon highland terrain sculpted by the Imbrium-basin impact. Associated high-titanium mare deposits were also emplaced in the lowlands at this time. The spectrally distinct, low-titanium "perched" lava pond (unit F) was then emplaced. Rima Bode I, associated with the probable source for this unit, meanders through this low-titanium basaltic unit, cutting across mantled highlands and disappearing abruptly at the edge of Sinus Aestuum. The youngest unit in the region is the low-titanium mare basalt of Sinus Aestuum (unit E, approximately 3.2 by old; Boyce and Johnson, 1978) which embays the mantled highlands and covers the distal portion of Rima Bode I.

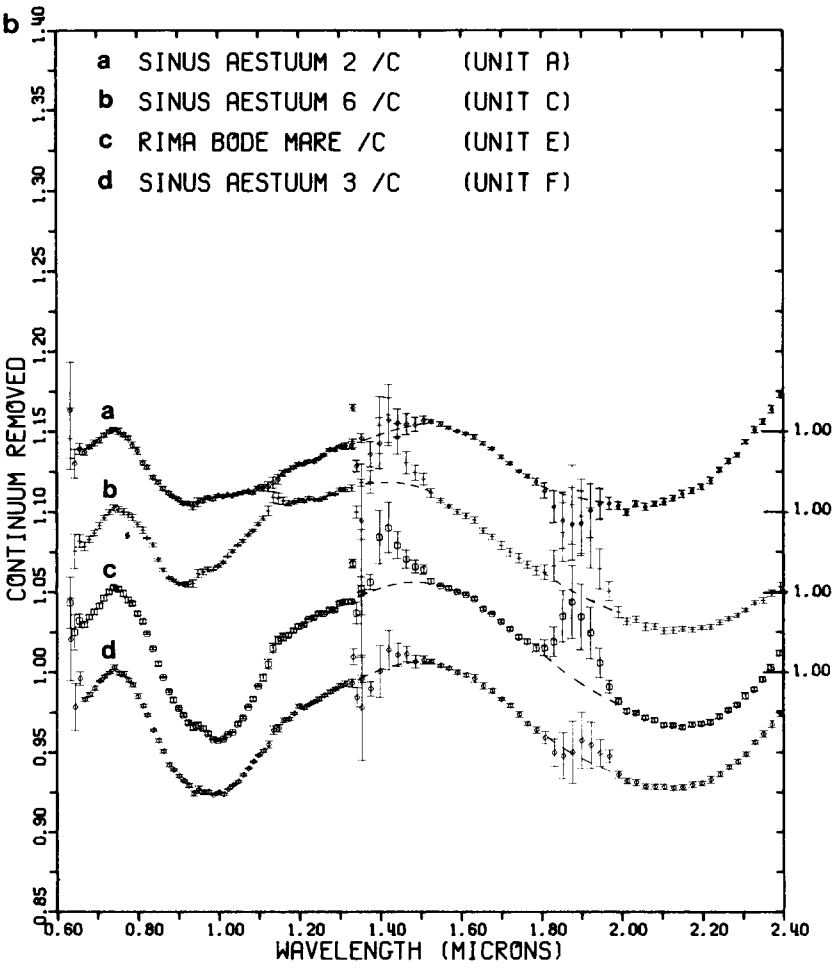

FIG. 8—*Continued.*

THE IDENTIFICATION OF ADDITIONAL LUNAR PYROCLASTIC MANTLING DEPOSITS

The unique telescopic spectral reflectance characteristics and low depolarized 3.8-cm radar backscatter of lunar pyroclastic mantling deposits were recognized by Pieters *et al.* (1973) and used to examine five areas of extremely low albedo. Subsequent laboratory spectral reflectance analyses of samples of orange glass and black spheres from Apollo 17 and green glass from Apollo 15 suggested that the "black spots" of Pieters *et al.* (1973) may be pyroclastic deposits which contain a significant component of black spheres comparable to those sampled at Taurus–Littrow (Adams *et al.*, 1974). We believe that the recognition of numerous varieties of volcanic glass samples, especially relatively high-albedo (e.g., green, yellow) glasses, suggests the existence of additional, unrecognized mantling deposits with albedos higher than those studied to date. Multispectral data presented by Johnson *et al.* (1977) and Davies *et al.* (1979) support this idea and suggest that the diverse spectral signatures of "dark mantle" deposits are indicative of the presence of glass-rich pyroclastic materials which are compositionally unrelated to those sampled by Apollo 17.

FIG. 9. Distribution of 35 areas examined for evidence of pyroclastic mantling material. The albedos of these areas are illustrated in this Lick Observatory full-moon photo (a) and their locations are plotted on the sketch map (b). Areas are numbered according to their appearance in Table III. ▲ = recognized regional mantling deposit; ● = recognized localized mantling deposit; ★ = possible regional mantling deposit; and ■ = other.

Since information obtained by radar primarily concerns the physical characteristics of the lunar surface, higher-albedo mantling deposits may be identifiable on 3.8-cm depolarized radar maps. To investigate this possibility we have examined 3.8-cm depolarized radar maps of the entire lunar nearside (Zisk *et al.*, 1974). Information on the location and morphology of known regional and localized lunar pyroclastic deposits was compiled (e.g., Carr, 1966; Schmitt *et al.*, 1967; Wilhelms, 1968; Ulrich, 1969; Wilhelms and McCauley, 1971; Lucchitta, 1972, 1973; Grolier, 1974; Head, 1974; Pieters *et al.*, 1975; Wilhelms and El-Baz, 1977; Zisk *et al.*, 1977; Hawke, *et al.*, 1979; Head and Wilson, 1979; Hawke and Head, 1980; Head *et al.*, 1980; Gaddis *et*

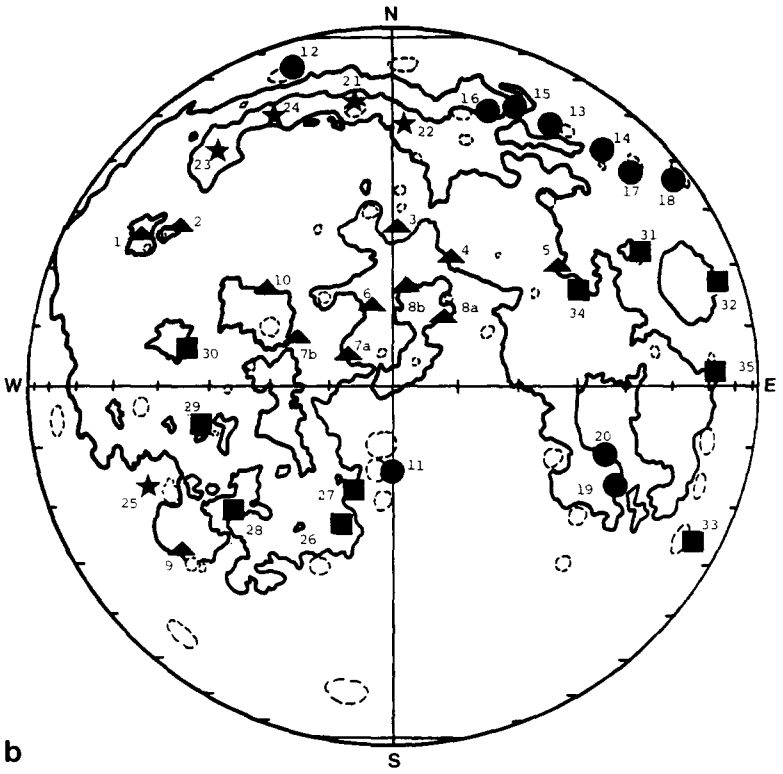

FIG. 9—*Continued.*

al., 1981) and it was established that all of the currently recognized, low-albedo (0.079–0.096; Pohn and Wildey, 1970) regional lunar pyroclastic mantling deposits exhibit relatively low depolarized 3.8-cm radar returns. In addition, a number of areas were identified which exhibit low depolarized 3.8-cm returns but are not characterized by low albedos (0.096–0.134; Pohn and Wildey, 1970); these areas are discussed further below. Each of the low-return areas was then studied on available photographs; sources include Lunar Orbiter IV, Consolidated Lunar Atlas, Apollo, and Lick Observatory full-moon photographs. For each site, attention was given to morphology, associated features (especially those which could be interpreted as volcanic source vents), and estimates of areal extent. The areas identified as recognized or possible pyroclastic deposits are presented in Table III.

Thirty-five lunar areas were subjected to a detailed examination for mantling material (Fig. 9 and Table III); these included 10 previously recognized regional deposits, 10 documented localized deposits, and 5 newly identified possible mantling deposits. In addition, 10 areas of relatively low radar return were identified which appear to be mare deposits (i.e., they have distinct boundaries which appear to embay the surrounding terrain) and are classified here as "other." The known regional deposits, which often have diffuse boundaries on both photographs and depolarized 3.8-cm radar maps, range in size from about 2500 up to 37,400 km^2. As discussed earlier, regional pyroclastic deposits are commonly situated on highland areas adjacent to major mare deposits and have associated sinuous rilles. The localized deposits (75 to 1000 km^2) are generally associated with endogenic dark-halo craters which are located

TABLE III

CHARACTERISTICS OF RECOGNIZED AND POSSIBLE LUNAR PYROCLASTIC MANTLING DEPOSITS

Name	Location	Areal extent (km^2)	Associated features and previous studies
	I. Recognized pyroclastic mantling deposits		
A. Regional			
1. Aristarchus	48 W, 24 N	37400	Vallis Schroteri (very large sinuous rille) and numerous smaller rilles with source depressions ("cobra-head" rilles) (Wilhelms and McCauley, 1971; Head, 1974; Zisk *et al.*, 1977)
2. Montes Harbinger	42 W, 20 N	5400	Numerous small rilles with source depressions (Wilhelms and McCauley, 1971; Head, 1974; Zisk *et al.*, 1977)
3. Palus Putredinis	0, 25 N	Up to 2800	Rima Hadley and fractures radial and concentric to Mare Imbrium (Wilhelms and McCauley, 1971; Hawke *et al*, 1979)
4. Sulpicius Gallus	10 E, 20 N	6000	Kidney-shaped depression, several irregular depressions and sinuous rilles (Wilhelms and McCauley, 1971; Head, 1974; Head *et al.*, 1980)
5. Taurus–Littrow	30 E, 20 N	4000	Rille with source depression near Littrow (Carr, 1966; Wilhelms and McCauley, 1971; Lucchitta, 1973; Head, 1974)
6. Rima Bode	3 W, 13 N	10000	Two rilles, to N and S (neither appears to be source) (Wilhelms, 1968; Wilhelms and McCauley, 1971; Head, 1974; Gaddis *et al.*, 1981)
7. S. Sinus Aestuum	7 W, 5 N	30000	Several small sinuous rilles and numerous dark-halo craters (Wilhelms and McCauley, 1971; Head, 1974)
8. Mare Vaporum	7 E, 10 N	10000	Rima Hyginus to SE and several smaller rilles (Wilhelms, 1968; Wilhelms and McCauley, 1971; Head, 1974)
9. Mare Humorum	40 W, 30 S	Up to 3000	Fractures concentric to Mare Humorum and two floor-fractured craters (Wilhelms and McCauley, 1971; Head, 1974; Pieters *et al.*, 1975)
10. Mt. Carpatus	25 W, 15 N	Up to 2500	Several short sinuous rilles with source depressions, some coalesced-crater chains, and numerous dark-halo craters (Schmitt *et al.*, 1967; Wilhelms and McCauley, 1971)
B. Localized			
11. Alphonsus	4 W, 13 S	Up to 80	Dark-halo craters aligned along fractures of floor-fractured crater (Wilhelms and McCauley, 1971; Head, 1974; Head and Wilson, 1979)
12. J. Herschel	41 W, 62 N	700	Coalesced dark-halo craters aligned along fractures of floor-fractured crater (Ulrich, 1969; Wilhelms and McCauley, 1971; Hawke and Head, 1980, McCord *et al.*, 1981)
13. Atlas	45 E, 47 N	N: 100 S: 250	Elongate craters aligned along fractures at floor-fractured crater (Grolier, 1974; Wilhelms and McCauley, 1971; Hawke and Head, 1980)
14. Franklin	48 E, 39 N	1000	A series of aligned elongated craters on crater floor (Wilhelms and McCauley, 1971; Grolier, 1974; Hawke and Head, 1980)
15. E of Aristoteles B	35 E, 50 N	575	Small fracture with elongated craters (no host crater) (Wilhelms and McCauley, 1971; Lucchitta, 1972; Hawke and Head, 1980)

TABLE III—*Continued*

Name	Location	Areal extent (km^2)	Associated features and previous studies
16. E of Aristoletes A	28 E, 50 N	1000	Partially filled irregular depression (no host crater) (Wilhelms and McCauley, 1971; Hawke and Head, 1980)
17. Messala	60 E, 39 N	700	Several small, aligned semicircular craters (Wilhelms and El-Baz, 1977; Hawke and Head, 1980)
18. Gauss	79 E, 36 N	Up to 350	Several small, elongated craters aligned along floor fracture (Wilhelms and El-Baz, 1977; Hawke and Head, 1980)
19. Bohnenberger	40 E, 16 S	75	Elongated craters aligned along crater floor fracture (Hawke and Head, 1980)
20. NE Nectaris	38 E, 12 S	250	Two short rilles with source depressions (Wilhelms and McCauley, 1971)
	II. Possible pyroclastic mantling deposits		
A. Regional			
21. Plato	10 W, 53 N	60000	Several sinuous rilles and coalesced crater chains located in highlands (some have associated mare ponds)
22. Montes Alpes	2 E, 48 N	60000	Alpine Valley with its associated sinuous rille and several other small highland sinuous rilles
23. W of Iridum	40 W, 42 N	85000	Numerous small highland sinuous rilles (some have associated mare ponds)
24. N of Iridum	35 W, 50 N	40000	Same as above
25. Gassendi	43 W, 15 S	45000	Several long sinuous rilles in mare to the east (*no* highland rilles evident)
B. Other			
26. Rupes Recta	9 W, 22 S	13500	Large sinuous rille with source depression to the west
27. Lassel	8 W, 16 S	200	None evident (Wilhelms and McCauley, 1971)
28. NE of Humorum	28 W, 21 S	1500	Few small fractures (no associated elongate craters)
29. Euclides	30 W, 8 S	3300	One small sinuous rille with source depression
30. SE, NE of Kepler	35 W, 8 N	SE: 2500 NE: 5000	Numerous small rilles, fractures, and crater chains
31. Macrobius	45 E, 23 N	11000	None evident
32. E Crisium	65 E, 15 N	2300	None evident
33. Petavius	60 E, 25 S	NE: 350 E: 200	Concentric fractures in crater floor (no associated craters) (Wilhelms and McCauley, 1971)
34. SE of Taurus–Littrow	31 E, 17 N	150	None evident (Wilhelms and McCauley, 1971)
35. W of Apollonius	53 E, 4 N	200	None evident (Wilhelms and McCauley, 1971)

along fractures or lineaments, sometimes in crater floors. Unlike the regional deposits, examples of localized deposits can be found which are not always situated near large mare deposits (e.g., Gauss, Messala).

The five regions which have been identified here as possible mantled areas have a number of characteristics in common with the known regional deposits. These possible pyroclastic deposits have diffuse boundaries on depolarized 3.8-cm radar maps, are large (40,000 to 85,000 km^2), occur on highland terrain, and, with the exception of the area west of Gassendi, have numerous nearby sinuous rilles which may represent volcanic source vents. A more detailed

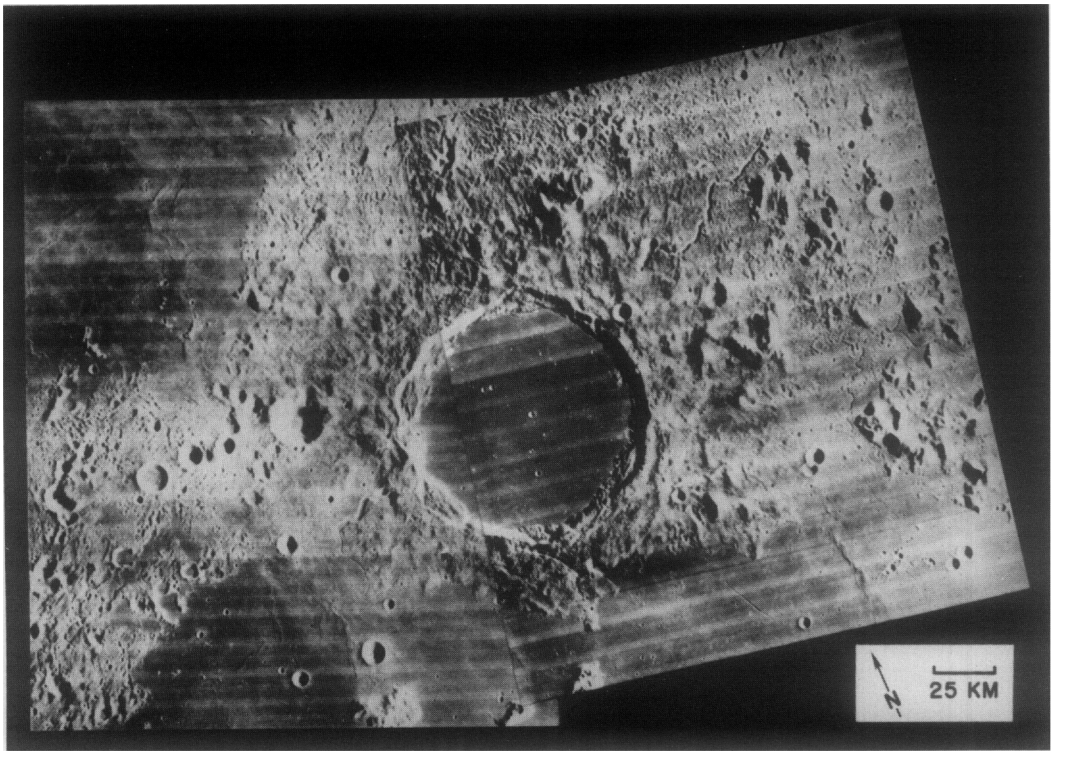

FIG. 10. High-resolution Lunar Orbiter IV (LO IV-134H3 and -122H3) photomosaic of the highland crater Plato.

look at the area near the crater Plato serves to illustrate some of these features.

Plato (Fig. 10) is a highland crater (d= 90 km) of Imbrian age which is located between Mare Frigoris and northern Mare Imbrium (M'Gonigle and Schleicher, 1972). Northern and southern portions of the ejecta deposit of this crater have been covered by mare deposits of late Imbrian age. Younger mare deposits, of Imbrian/Eratosthenian age, have flooded the interior of Plato and several sites along the perimeter of the area of interest here (Fig. 11).

Polarized and depolarized 3.8-cm radar images of Plato are presented in Fig. 12. As delineated in Fig. 11, a large portion (about 60,000 km^2) of the highland terrain surrounding Plato is distinguished by a relatively low 3.8-cm depolarized radar return (Thompson and Zisk, 1972; Thompson *et al.*, 1978). It is suggested that this low depolarized return at 3.8-cm wavelengths may be evidence of a mantling layer of fine-grained pyroclastic material of intermediate albedo. This hypothesis is supported by the smooth surface of the local highland terrain, by the lower-than-normal albedo for this terra surface (0.114–0.127, as compared to 0.127 or higher for most of the lunar highlands; Pohn and Wildey, 1970), and by the presence of numerous sinuous rilles and coalesced crater chains which may represent source vents for pyroclastic materials. At least one of the larger sinuous rilles (Rima Plato I) has been cited as a possible source for a small (area = 28 km^2) mantling deposit (M'Gonigle and Schleicher, 1972). This late Imbrian mantling unit is one of eight small "probable pyroclastic" deposits (M'Gonigle and Schleicher, 1972) which are

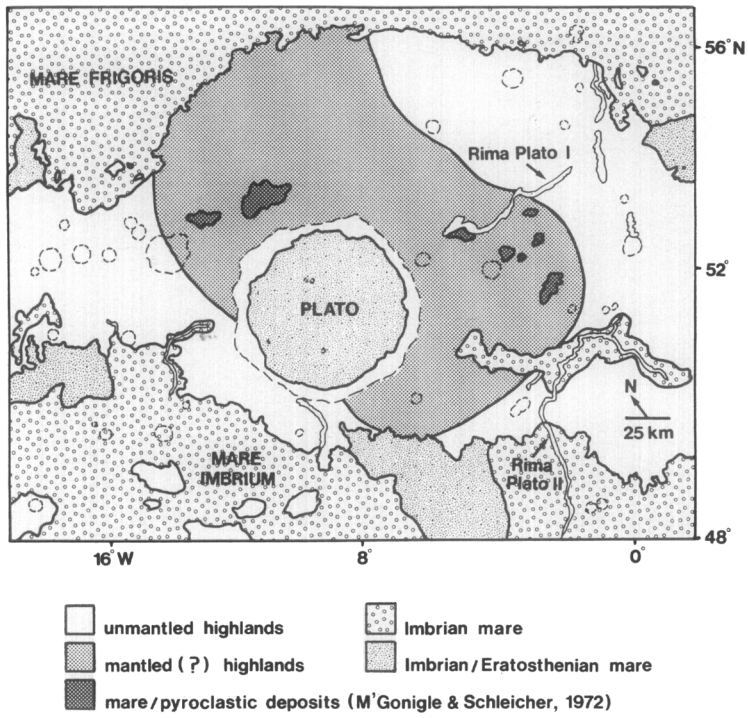

FIG. 11. Distribution of geologic units of the Plato region.

characterized as having moderately low albedos and irregular outlines, and as thinly mantling older topography.

Although regional lunar pyroclastic mantling deposits were readily identifiable as low-return areas on 3.8-cm depolarized radar maps, the localized deposits were more difficult to distinguish. Fewer than half of the known localized deposits could be identified on depolarized radar images. There are two possible explanations for this difficulty: either their components do not significantly attenuate the 3.8-cm radar signals or the spatial resolution (about 2 km) of the 3.8-cm radar data is inadequate to resolve these small surface units. Since it is not known whether localized pyroclastic deposits have been sampled, their chemical compositions are as yet poorly constrained. Spectral reflectance data for several of these units suggest that their compositions differ from those of regional pyroclastic deposits; they may not contain significant quantities of glassy iron- and titanium-rich materials (Lucey *et al.*, 1984). Alternatively, only 3 of the 11 dark-halo craters of Alphonsus crater are apparent on these radar maps. Since deposits associated with these 3 endogenic craters form a relatively tight cluster, their combined thickness and areal extent (about 80 km^2) may be sufficient to produce a low 3.8-cm return which can be resolved on depolarized radar maps. This limitation in resolution suggests that pyroclastic units which can be identified using 3.8-cm radar data alone are most likely to be regional or relatively large (i.e., coalesced or overlapping) localized mantling deposits. Smaller localized units may best be identified using high-resolution photography of the lunar surface, with an emphasis placed on examination of small craters aligned along fractures or lineations.

Additional evidence bearing on the presence of pyroclastic mantling material in the five new areas proposed here may come

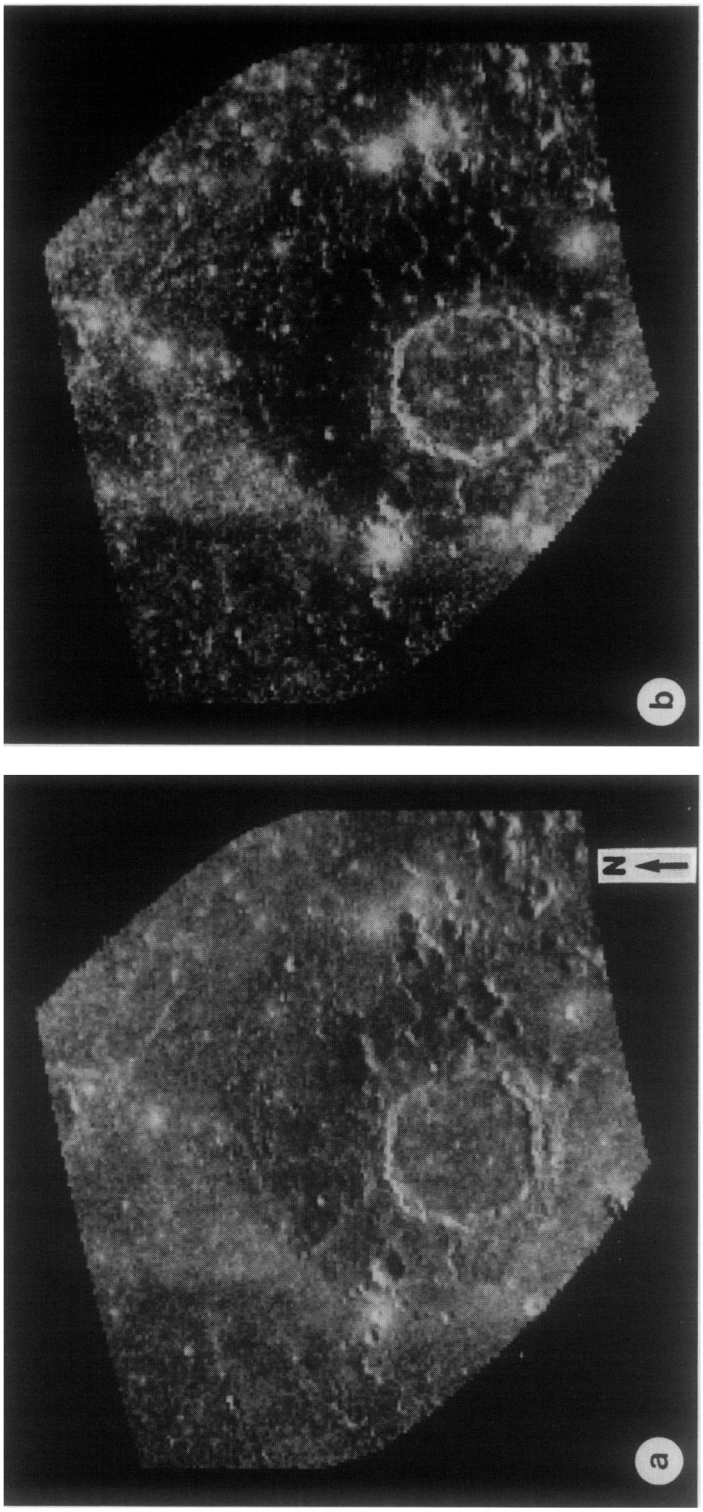

FIG. 12. (a) Polarized and (b) depolarized 3.8-cm radar backscatter maps of Plato (ZAC 6.30; Zisk *et al.*, 1974).

from further near-infrared spectral reflectance studies. If these areas are indeed mantled by Fe-bearing glass-rich pyroclastic deposits, their spectra should exhibit broad, relatively shallow 1.0-μm absorption bands. At present, this 1.0-μm Fe-bearing glass band is difficult to distinguish from a 1.0-μm olivine band. However, one characteristic spectral feature of Fe-bearing glasses is the presence of an absorption band near 2.0 μm; this band has been attributed to Fe^{+2} on tetrahedral coordination sites (Adams, 1975). The mineral olivine has no such 2.0-μm absorption band. Acquisition of high-resolution spectra of lunar pyroclastic mantling deposits out to wavelengths beyond 2.0 μm may therefore permit a distinction between Fe-bearing glasses and olivine to be made.

SUMMARY AND CONCLUSIONS

Regional lunar pyroclastic deposits are products of explosive fire-fountaining eruptions which may have been associated with some of the early mare-filling volcanic episodes. These mantling deposits, commonly located on highland areas near several of the major lunar maria, are characterized as low-albedo units which appear to cover and subdue the features of the underlying terrain. Homogeneous, Fe-bearing volcanic glasses and partially crystallized spheres have been recognized as important constituents of samples returned from lunar pyroclastic mantling deposits (e.g., Delano and Livi, 1981b; Delano and Lindsley, 1983a, b). The surfaces of these pyroclastic components are coated with volatile elements believed to have been condensed from gases involved in an explosive eruption (e.g., Wasson *et al.*, 1976); these surface-correlated volatile concentrations provide striking contrast to the volatile-depleted bulk lunar composition (e.g., Ganapathy and Anders, 1974). Examination of the nature and distribution of lunar pyroclastic mantling deposits may therefore lead to a better understanding of the locations and compositions of their source regions, and the eruption mechanisms of lunar magmas.

Remote sensing data currently provide us with the best means of identifying and characterizing lunar mantling deposits. In this paper, we have summarized current morphological, 3.8-cm radar, and spectral reflectance data for lunar pyroclastic deposits. More specifically, information on the location, areal extent, and associated features of previously recognized regional and localized mantling deposits has been consolidated and presented. The very weak depolarized 3.8-cm radar signatures of all of the known regional deposits have been documented; low backscatter on the 3.8-cm depolarized radar maps has been attributed previously to the fine-grained, loosely consolidated nature of these deposits (e.g., Pieters *et al.*, 1973; Zisk *et al.*, 1977). Several new near-infrared reflectance spectra for known regional pyroclastic mantling deposits have also been presented; these spectra support a previous interpretation that mantling units have unique spectral signatures which are indicative of a significant Fe-bearing volcanic glass component. To further document the utility of a variety of remote sensing data in characterizing regional pyroclastic mantling deposits, 3.8-cm radar, multispectral vidicon, and spectral reflectance data for the Rima Bode region have been presented and used to interpret its geologic history. Furthermore, the recognition of relatively high-albedo (e.g., green, yellow) volcanic glasses in returned lunar samples suggest the existence of additional, previously unrecognized mantling deposits with albedos higher than those studied to date. To identify such higher-albedo mantling deposits, the very weak depolarized 3.8-cm radar signature of recognized regional mantling deposits has been utilized. As a result, five new possible mantled areas have been identified; these areas all have anomalously low 3.8-cm radar return and appear to be mantled by a smooth-surfaced, intermediate- to high-albedo deposit.

A number of conclusions may be derived from this analysis of the remote sensing characteristics of lunar pyroclastic mantling deposits:

(1) Spectral absorption band analysis and albedo considerations suggest that Fe-bearing volcanic glass is present not only in previously sampled lunar pyroclastic mantling deposits (e.g., Apollo 17/Taurus–Littrow, Apollo 15/Palus Putredinis) but in several other regional mantling deposits as well. This interpretation is supported by analyses of multispectral data presented by Johnson *et al.* (1977) and Davies *et al.* (1979). These authors suggest that the diverse spectral signatures of "dark mantle" deposits indicate the presence of glass-rich pyroclastic materials which have chemical/physical characteristics which differ from the orange glasses sampled by Apollo 17 at Taurus–Littrow.

(2) On the basis of photogeologic, radar, and spectral analyses, the Rima Bode region is demonstrated to be mantled by a low-albedo pyroclastic mantling deposit which is compositionally similar to the high-titanium, glass-rich deposit sampled at Taurus–Littrow. If, as Head (1974) suggested for the Apollo 17 site, the emplacement of pyroclastics in the Rima Bode area was associated with high-titanium volcanism, then mare basalts of similar composition would underlie the low-titanium maria which are currently observable in Sinus Aestuum.

(3) All of the previously recognized regional pyroclastic mantling deposits have very low depolarized 3.8-cm radar signatures. We believe that these backscatter characteristics reflect the smooth-surfaced, fine-grained, unconsolidated physical character of mantling deposits and that they are relatively independent of albedo. The low depolarized 3.8-cm radar signature of mantling deposits is therefore a valid tool for identifying additional pyroclastic deposits which have albedos higher than those studied to date.

(4) Examination of all of the 3.8-cm depolarized radar imagery of the lunar nearside has revealed several low-return areas which are not characterized by low albedos. Five of these areas consist of smooth-surfaced highland terrains with nearby rilles and/or irregular depressions which may represent source vents for pyroclastic volcanism. These five areas may therefore be mantled by pyroclastic deposits with intermediate to high albedos. The acquisition and interpretation of additional spectral reflectance data for the deposits in these new areas may help to corroborate their pyroclastic origin.

ACKNOWLEDGMENTS

One of the authors (L.R.G.) was supported by a Title IX Fellowship while at Brown University. In addition, this research was supported by NASA Grants NAGW-28 and NAWG-37 (C.M.P.), and NSG-7323, NSG-7812, and NAGW-237 (B.R.H.). We thank Pam Owensby for help in the collection and reduction of spectral reflectance data. Insightful comments on an earlier version of this manuscript by Don E. Wilhelms and John W. Delano are gratefully acknowledged.

REFERENCES

ADAMS, J. B. (1974). Visible and near-infrared diffuse reflectance spectra as applied to remote sensing of solid objects in the solar system. *J. Geophys. Res.* **79**, 4829–4836.

ADAMS, J. B. (1975). Interpretation of visible and near-infrared reflectance spectra of pyroxenes and other rock-forming minerals. In *Infrared and Raman Spectroscopy of Lunar and Terrestrial Minerals* (C. Karr, Jr., Ed.), pp. 90–116. Academic Press, New York.

ADAMS, J. B., AND T. B. MCCORD (1970). Remote sensing of lunar surface mineralogy: Implications from visible and near-infrared reflectivity of Apollo 11 samples. *Proc. Lunar Sci. Conf. Apollo 11*, 1937–1945.

ADAMS, J. B., AND T. B. MCCORD (1971). Optical properties of mineral separates, glass, and anorthositic fragments from Apollo mare samples. *Proc. Lunar Sci. Conf. 2nd*, 2183–2195.

ADAMS, J. B., AND T. B. MCCORD (1972). Electronic spectra of pyroxenes and interpretation of telescopic spectral reflectivity curves of the Moon. *Proc. Lunar Sci. Conf. 3rd*, 3021–3034.

ADAMS, J. B., C. PIETERS, AND T. B. MCCORD (1974). Orange glass: Evidence for regional deposits of pyroclastic origin on the Moon. *Proc. Lunar Sci. Conf. 5th*, 171–186.

ALEXANDER, E. C., JR., M. R. COSCIO, JR., J. C. DRAGON, AND K. SAITO (1980). K/Ar dating of lunar soils IV: Orange glass from 74220 and agglutinates from 14259 and 14163. *Proc. Lunar Planet. Sci. Conf. 11th,* 1663–1677.

ANDRE, C. G., M. J. BIELEFELD, E. ELIASON, L. A. SODERBLOM, I. ADLER, AND J. A. PHILPOTTS, (1977). Lunar surface chemistry: A new imaging technique. *Science (Washington, D.C.)* **197,** 986–989.

ARNOLD, J., A. E. METGER, AND R. C. REEDY (1977). Computer-generated maps of lunar composition from gamma-ray data. *Proc. Lunar Sci. Conf. 8th,* 945–948.

Basaltic Volcanism Study Project (1981). *Basaltic Volcanism on the Terrestrial Planets.* Pergamon, Elmsford, New York.

BELL, P. M., H. K. MAO, AND R. A. WEEKS (1976). Optical spectra and electron paramagnetic resonance of lunar and synthetic glasses: A study of the effects of controlled atmosphere, composition, and temperature. *Proc. Lunar Sci. Conf. 7th,* 2543–2559.

BIELEFELD, M., C. ANDRE, E. ELIASON, P. CLARK, I. ADLER, AND J. TROMBKA (1977). Imaging of lunar surface chemistry from orbital X-ray data. *Proc. Lunar Sci. Conf. 8th,* 901–908.

BOYCE, J. M., AND D. A. JOHNSON (1978). Ages of flow units in the far eastern maria and implications for basin-filling history. *Proc. Lunar Planet. Sci. Conf. 9th,* 3275–3283.

BURNS, R. G. (1970a). *Mineralogical Applications of Crystal Field Theory.* Cambridge Univ. Press, London.

BURNS, R. G. (1970b). Crystal field spectra and evidence of cation ordering in olivine minerals. *Amer. Mineral.* **55,** 1602–1632.

BURNS, R. G. (1974). The polarized spectra of iron in silicates: Olivine, a discussion of neglected contributions from Fe ions in M(1) sites. *Amer. Mineral.* **59,** 625–629.

BUTLER, P., JR. (1978). Recognition of lunar glass droplets produced directly from endogenous liquids: The evidence from S–Zn coatings. *Proc. Lunar Planet. Sci. Conf. 9th,* 1459–1471.

CARR, M. H. (1966). *Geologic Map of the Mare Serenitatis Region of the Moon,* USGS Misc. Geol. Inv. Map I-489.

CERNAN, E. A., R. E. EVANS, AND H. SCHMITT (1972). *Apollo 17 technical air-to-ground voice transcription,* MSC-07629.

CHARETTE, M. P., T. B. MCCORD, C. PIETERS, AND J. B. ADAMS (1974). Application of remote spectral reflectance measurements to lunar geology classification and determination of titanium content of lunar soils. *J. Geophys. Res.* **79,** 1606–1613.

CHARETTE, M. P., L. A. SODERBLOM, J. B. ADAMS, M. J. GAFFEY, AND T. B. MCCORD (1976). Age–color relationships in the lunar highlands. *Proc. Lunar Sci. Conf. 7th,* 2579–2592.

CHOU, C. L., W. V. BOYNTON, L. L. SUNDBERG, AND J. T. WASSON (1975). Volatiles on the surface of Apollo 15 green glass and trace element distributions among Apollo 15 soils. *Proc. Lunar Sci. Conf. 6th,* 1701–1727.

DAVIES, D. W., T. V. JOHNSON, AND D. L. MATSON (1979). Lunar multispectral mapping at 2.26 microns: First results. *Proc. Lunar Planet. Sci. Conf. 10th,* 1819–1828.

DELANO, J. W. (1979). Apollo 15 green glass: Chemistry and possible origin. *Proc. Lunar Planet. Conf. 10th,* 275–300.

DELANO, J. W., AND D. H. LINDSLEY (1983a). Mare volcanic glasses from Apollo 17. *Lunar Planet. Sci. XIV,* 156–157.

DELANO, J. W., AND D. H. LINDSLEY (1983b). Mare glasses from Apollo 17: Constraints on the Moon's bulk composition. *Proc. Lunar Planet. Sci. Conf. 14th J. Geophys. Res.* **88,** (Suppl.), B3–B16.

DELANO, J. W., AND K. LIVI (1981a). Mare volcanic glasses: A tale of two arrays. *Lunar Planet. Sci. XII,* 226–228.

DELANO, J. W., AND K. LIVI (1981b). Lunar volcanic glasses and their constraints on mare petrogenesis. *Geochim. Cosmochim. Acta* **45,** 2137–2149.

DELANO, J. W., S. R. TAYLOR, AND A. E. RINGWOOD (1980). Composition and structure of the deep lunar interior. *Lunar Planet. Sci. XI,* 225–227.

FARR, T. G., B. A. BATES, R. L. RALPH, AND J. B. ADAMS (1980). Effects of overlapping optical absorption bands of pyroxene and glass on the reflectance spectra of lunar soils. *Proc. Lunar Planet. Sci. Conf. 11th,* 719–729.

GADDIS, L. R., J. B. ADAMS, B. R. HAWKE, J. W. HEAD, T. B. MCCORD, C. M. PIETERS, AND S. H. ZISK (1981). Characterization and distribution of pyroclastic units in the Rima Bode region of the Moon. *Lunar Planet. Sci. XII,* 318–320.

GADDIS, L. R., AND J. W. HEAD (1981). Distribution and volumes of lava ponds in the Orientale region of the Moon. *Lunar Planet. Sci. XII,* 321–323.

GANAPATHY, R., AND E. ANDERS (1974). Bulk composition of the moon and earth, estimated from meteorites. *Proc. Lunar Sci. Conf. 5th,* 1181–1206.

GROLIER, M. J. (1974). *Geologic Map of the Geminus Quadrangle of the Moon,* USGS Misc. Geol. Inv. Map I-841.

HAWKE, B. R., AND J. F. BELL (1981). Remote sensing studies of lunar dark-halo impact craters: Preliminary results and implications for early mare volcanism. *Proc. Lunar Planet. Sci. Conf. 12B,* 665–678.

HAWKE, B. R., AND J. W. HEAD (1980). Small dark-mantle deposits of possible pyroclastic origin: Geologic setting, composition, and relation to regional stratigraphy. *Lunar Planet. Sci. XI,* 416–417.

HAWKE, B. R., P. G. LUCEY, T. B. MCCORD, C. M. PIETERS, AND J. W. HEAD (1983). Spectral studies of the Aristarchus region: Implications for the composition of the lunar crust. *Lunar Planet. Sci. XIV*, 289–290.

HAWKE, B. R., D. MACLASKEY, T. B. MCCORD, J. B. ADAMS, J. W. HEAD, C. M. PIETERS, AND S. H. ZISK (1979). Multispectral mapping of the Apollo 15–Apennine region: The identification and distribution of regional pyroclastics. *Proc. Lunar Planet. Sci. Conf. 10th*, 2995–3015.

HAZEN, R. M., P. M. BELL, AND H. K. MAO (1978). Effects of compositional variation on absorption spectra of lunar pyroxenes. *Proc. Lunar Planet. Sci. Conf. 9th*, 2919–2934.

HEAD, J. W. (1974). Lunar dark-mantle deposits: Possible clues to the distribution of early mare deposits. *Proc. Lunar Sci. Conf. 5th*, 207–222.

HEAD, J. W., J. B. ADAMS, B. R. HAWKE, T. B. MCCORD, C. M. PIETERS, AND S. H. ZISK (1980). Sulpicius Gallus pyroclastic deposits, southwestern Serenitatis region of the Moon. *Lunar Planet. Sci. XI*, 418–420.

HEAD, J. W., AND L. WILSON (1979). Alphonsus-type dark-halo craters: Morphology, morphometry and eruption conditions. *Proc. Lunar Planet. Sci. Conf. 10th*, 2861–2897.

HEIKEN, G. H., D. S. MCKAY, AND P. W. BROWN (1974). Lunar deposits of possible pyroclastic origin. *Geochim. Cosmochim. Acta* **38,** 1703–1718.

HUNEKE, J. C., JR. (1978). ^{40}Ar–^{39}Ar microanalysis of single 74220 glass balls and 72435 breccia clasts. *Proc. Lunar Planet. Sci. Conf. 9th*, 2345–2362.

JOHNSON, T. V., J. A. MOSHER, AND D. L. MATSON (1977). Lunar spectral units: A northern hemisphere mosaic. *Proc. Lunar Sci. Conf. 8th*, 1013–1028.

LSPET (1973). Apollo 17 lunar samples: Chemical and petrographic description. *Science (Washington, D.C.)* **182,** 659–672.

LUCCHITTA, B. K. (1972). *Geologic Map of the Aristoteles Quadrangle of the Moon*, USGS Map I-725.

LUCCHITTA, B. K. (1973). Photogeology of the dark material in the Taurus–Littrow region of the Moon. *Proc. Lunar Sci. Conf. 4th*, 149–162.

LUCCHITTA, B. K., AND H. H. SCHMITT (1974). Orange material in the Sulpicius Gallus formation at the southwestern edge of Mare Serenitatis. *Proc. Lunar Sci. Conf. 5th*, 223–234.

LUCEY, P. G., L. R. GADDIS, J. F. BELL, AND B. R. HAWKE (1984). Near-infrared spectral reflectance studies of localized dark mantle deposits. *Lunar Planet. Sci. XV*, 495–496.

MCCORD, T. B., M. P. CHARETTE, T. V. JOHNSON, L. A. LEBOFSKY, C. M. PIETERS, AND J. B. ADAMS (1972). Lunar spectral types. *J. Geophys. Res.* **77,** 1349–1359.

MCCORD, T. B., R. N. CLARK, B. R. HAWKE, L. A. MCFADDEN, P. D. OWENSBY, C. M. PIETERS, AND J. B. ADAMS (1981). Moon: Near-infrared spectral reflectance, a first good look. *J. Geophys. Res.* **86,** 10883–10892.

MCCORD, T. B., C. PIETERS, AND M. A. FEIERBERG (1976). Multispectral mapping of the lunar surface using ground-based telescopes. *Icarus* **29,** 1–34.

MCGETCHIN, T. R., AND G. W. ULLRICH (1973). Zenoliths in maars and diatremes with inferences for the Moon, Mars and Venus. *J. Geophys. Res.* **78,** 1833–1853.

MEYER, C. JR., D. S. MCKAY, D. H. ANDERSON, AND P. BUTLER (1975). The source of sublimates on the Apollo 15 green and Apollo 17 orange glass samples. *Proc. Lunar Sci. Conf. 6th*, 1673–1699.

M'GONIGLE, J. W., AND D. SCHLEICHER (1972). *Geologic Map of the Plato Quadrangle of the Moon*, USGS Map I-701.

PETTENGILL, G. H., S. H. ZISK, AND T. W. THOMPSON (1974). The mapping of lunar radar scattering characteristics. *Moon* **10,** 3–16.

PIETERS, C. (1977). Characterization of lunar mare basalt types. I. Spectral classification of fresh mare craters. *Proc. Lunar Sci. Conf. 8th*, 1037–1048.

PIETERS, C. M. (1978). Mare basalt types on the front side of the moon: A summary of spectral reflectance data. *Proc. Lunar Planet. Sci. Conf. 9th*, 2825–2849.

PIETERS, C. M. (1982). Copernicus crater central peak: Lunar mountain of unique composition. *Science (Washington, D.C.)* **215,** 59–61.

PIETERS, C. M., J. W. HEAD, T. B. MCCORD, J. B. ADAMS, AND S. H. ZISK (1975). Geochemical and geological units of Mare Humorum: Definition using remote sensing and lunar sample information. *Proc. Lunar Sci. Conf. 6th*, 2689–2710.

PIETERS, C. M., T. B. MCCORD, M. P., CHARETTE, AND J. B. ADAMS (1974). Lunar surface: Identification of the dark mantling material in the Apollo 17 soil samples. *Science (Washington, D.C.)* **183,** 1191–1194.

PIETERS, C. M., T. B. MCCORD, S H. ZISK, AND J. B. ADAMS (1973). Lunar black spots and the nature of the Apollo 17 landing area. *J. Geophys. Res.* **78,** 5867–5875.

PIETERS, C. M., AND S. SMREKAR (1982). *Atlas of Lunar Spectral Reflectance, 0.7–2.5 Microns*, Brown University Planetary Geology Document.

POHN, H. A., AND R. L. WILDEY (1970). *A Photoelectric–Photographic Study of the Normal Albedo of the Moon*, USGS Prof. Paper 599-E, Plate 1.

SCHMITT, H. H., N. J. TRASK, AND E. M. SHOEMAKER (1967). *Geologic Map of the Copernicus Quadrangle of the Moon*, USGS Misc. Geol. Inv. Map I-515.

SCHONFELD, E. (1981). High spatial resolution Mg/Al maps of the western Crisium and Sulpicius Gallus regions. *Proc. Lunar Planet. Sci. Conf. 12B*, 809–816.

SCHONFELD, E., AND M. J. BIELEFELD (1978). Correlation of dark-mantle deposits with Mg/Al ratios. *Proc. Lunar Planet. Sci. Conf. 9th,* 3037–3048.

SCHULTZ, P. H. (1976). *Moon Morphology.* Univ. of Texas Press, Austin.

SCOTT, D. H., B. K. LUCCHITTA, AND M. H. CARR (1972). *Geologic Maps of the Taurus–Littrow Region of the Moon,* USGS Misc. Geol. Inv. Map I-800.

SINGER, R. B. (1981). Near-infrared spectral reflectance of mineral mixtures: Systematic combinations of pyroxenes, olivine, and iron oxides. *J. Geophys. Res.* **86,** 7967–7982.

STONE, C. D., L. A. TAYLOR, D. S. MCKAY, AND R. V. MORRIS (1982). Ferromagnetic resonance intensity: A rapid method for determining lunar glass bead origin. *Proc. Lunar Planet. Sci. Conf. 13th, J. Geophys. Res.* **87,** (Suppl.), A182–A196.

THOMPSON, T. W. (1979). A review of Earth-based radar mapping of the Moon. *Moon Planets* **20,** 179–198.

THOMPSON, T. W., T. V. JOHNSON, D. L. MATSON, R. S. SAUNDERS, R. W. SHORTHILL, S. H. ZISK, H. J. MOORE, AND G. G. SCHABER (1978). Unusual remote sensing signatures of Montes Jura and crater Plato. *Lunar Planet. Sci. Conf. IX,* 1164–1165.

THOMPSON, T. W., H. MASURSKY, R. W. SHORTHILL, G. L. TYLER, AND S. H. ZISK (1974). A comparison of infrared geologic mapping of lunar craters. *Moon* **10,** 87–117.

THOMPSON, T. W., AND S. H. ZISK (1972). Radar mapping of lunar surface roughness (Chap. 1c). In *Thermal Characteristics of the Moon* (J. Lucas, Ed.), from *Progress in Aeronautics and Astronautics,* pp. 83–117. MIT Press, Cambridge, Mass.

ULRICH, G. E. (1969). *Geologic Map of the J. Herschel Quadrangle of the Moon,* USGS Misc. Geol. Inv. Map I-604.

WASSON, J. T., W. V. BOYNTON, G. W. KALLEMEYN, L. L. SUNDBERG, AND C. M. WAI (1979). Volatile compounds released during lunar lava fountaining. *Proc. Lunar Planet. Sci. Conf. 7th,* 1583–1595.

WHITAKER, E. A. (1972). Lunar color boundaries and their relationship to topographic features: A preliminary survey. *Moon* **4,** 348–355.

WILHELMS, D. E. (1968). *Geologic map of the Mare Vaporum quadrangle of the Moon,* USGS Misc. Geol. Inv. Map I-548.

WILHELMS, D. E. (1970). *Summary of Lunar Stratigraphy–Telescopic Observations.* USGS Prof. Paper 599-F.

WILHELMS, D. E., AND F. EL-BAZ (1977). *Geologic Map of the East Side of the Moon,* USGS Misc. Geol. Inv. Map I-948.

WILHELMS, D. E., AND J. F. MCCAULEY (1971). *Geologic Map of the Near Side of the Moon,* USGS Misc. Geol. Inv. Map I-703.

WILSON, L., AND J. W. HEAD (1981). Ascent and eruption of basaltic magma on the Earth and Moon. *J. Geophys. Res.* **78,** 2971–3001.

ZISK, S. H., C. A. HODGES, H. J. MOORE, R. W. SHORTHILL, T. W. THOMPSON, E. A. WHITAKER, AND D. E. WILHELMS (1977). The Aristarchus–Harbinger region of the Moon: Surface geology and history from recent remote-sensing observations. *Moon* **17,** 59–99.

ZISK, S. H., G. H. PETTENGILL, AND G. W. CATUNA (1974). High-resolution radar map of the lunar surface at 3.8-cm wavelength. *Moon* **10,** 17–50.